

Method for the Large-Scale Synthesis of Multifunctional 1,4-Dihydro-pyrrolo[3,2-*b*]pyrroles

Mariusz Tasiar, Olena Vakuliuk, Daiki Koga, Beata Koszarna, Krzysztof Górski, Marek Grzybowski, Łukasz Kielesiński, Maciej Krzeszewski, and Daniel T. Gryko*



Cite This: *J. Org. Chem.* 2020, 85, 13529–13543



Read Online

ACCESS |



Metrics & More



Article Recommendations



Supporting Information

ABSTRACT: A thorough investigation has enabled the optimization of the synthesis of 1,4-dihydro-pyrrolo[3,2-*b*]pyrroles. Although salts of such metals as vanadium, niobium, cerium, and manganese were found to facilitate the formation of 1,4-dihydro-pyrrolo[3,2-*b*]pyrroles from amines, aldehydes, and diacetyl, we confirmed that iron salts are the most efficient catalysts. The conditions identified (first step: toluene/AcOH = 1:1, 1 h, 50 °C; second step: toluene/AcOH = 1:1, Fe(ClO₄)₃·H₂O, 16 h, 50 °C) resulted in the formation of tetraarylpyrrolo[3,2-*b*]pyrroles in a 6–69% yield. For the first time, very electron-rich substituents (4-Me₂NC₆H₄, 3-(OH)C₆H₄, pyrrol-2-yl) originating from aldehydes and sterically hindered substituents (2-ClC₆H₄, 2-BrC₆H₄, 2-CNC₆H₄, 2-(CO₂Me)C₆H₄, 2-(TMS-C≡C)C₆H₄) present on anilines can be appended to the pyrrolo[3,2-*b*]pyrrole core. It is now also possible to prepare 1,4-dihydropyrrolo[3,2-*b*]pyrroles bearing an ordered arrangement of *N*-substituents and *C*-substituents ranging from coumarin, quinoline, phthalimide to truxene. These advances in scope enable independent regulations of many desired photophysical properties, including the Stokes shift value and emission color ranging from violet-blue through deep blue, green, yellow to red. Simultaneously, the optimized conditions have finally allowed the synthesis of these extremely promising heterocycles in amounts of more than 10 g per run without a concomitant decrease in yield or product contamination. Empowered with better functional group compatibility, novel derivatization strategies were developed.



INTRODUCTION

The rising interest in conjugated heterocycles composed of two or more rings has its origin in organic electronics. Among various systems,^{1,2} heteropentalenes^{3–5} attract particular attention, with a special focus on thieno[3,2-*b*]thiophene.^{6–10} This chromophore, especially when embedded into larger, π -extended scaffolds, has been employed in research ranging from active high-efficiency organic solar cells¹¹ to mechanosensitive fluorescent probes.¹² 1,4-Dihydro-pyrrolo[3,2-*b*]pyrroles are exceptionally electron-rich heteropentalenes, the chemistry of which has been developing very slowly for many years due to the lack of an efficient synthesis methodology.¹³ This situation changed dramatically in 2013, when we serendipitously found a method that allows rapid access to 1,4-dihydro-tetraarylpyrrolo[3,2-*b*]pyrroles (TAPPs).¹⁴ Since then, TAPPs have found multiple applications in research related to studying symmetry-breaking in the excited state,¹⁵ two-photon absorption,¹⁶ solvatofluorochromism,^{13c,d} direct solvent probing via H-bonding interactions,¹⁷ photochromic analysis of halocarbons,¹⁸ organic field-effect transistors,¹⁹ dye-sensitized solar cells,²⁰ bulk heterojunction organic solar cells,²¹ organic light-emitting diodes,²² resistive memory devices,²³ aggregation-

induced emission,²⁴ and MOFs.²⁵ It has been also shown that TAPPs are an excellent platform for the synthesis of the π -expanded heteroanalogues of polycyclic aromatic hydrocarbons.²⁶ Access to these aza-nanographenes hinges on the ability to prepare 1,4-dihydro-tetraarylpyrrolo[3,2-*b*]pyrroles possessing a suitable substitution pattern. In spite of significant efforts, many important functionalities have been so far incompatible with the multicomponent reaction leading to TAPPs. Simultaneously, the consequence of a growing interest in TAPPs is the increased demand for large quantities of these compounds. The possibility of large-scale preparation is also appreciated if industrial applications are seriously considered. Since our initial discovery,^{14a} the reaction conditions for the multicomponent reaction of primary aromatic amines, aromatic aldehydes, and diacetyl, leading to TAPPs, have evolved. A few

Received: July 13, 2020

Published: September 10, 2020



years ago, we found that the addition of *p*-toluenesulfonic acid to the reaction mixture significantly increased the yields, with some limitations regarding the starting materials.^{14b} More recently, we developed an improved procedure with an iron salt as the catalyst, leading to TAPPs in up to 77% yield with a reasonably broad substrate tolerance.²⁷ The huge advantages of this protocol are its simplicity, the use of cheap starting materials, and straightforward workup as most TAPPs precipitate directly from the reaction mixture. Routinely, this methodology was tested on the scale of 1.0 mmol of diacetyl, with an amine, aldehyde, and diacetyl used in a 2:2:1 molar ratio, with 6 mol % of catalyst and carried out in an open flask. Increasing the scale by a factor of 4–5 usually leads to negligible changes in the reaction outcome; however, attempting to scale up this process even further (to 40 mmol of diacetyl) resulted in a significant drop in reaction yield (by a factor of at least 3) and the product being contaminated with the unreacted Schiff base. Reproducibility is a common problem associated with the scaling-up of chemical processes developed on a laboratory scale. The increasing interest in pyrrolo[3,2-*b*]pyrrole chemistry undoubtedly hinges upon better access to these heterocyclic compounds, and the problem of scalability might significantly hamper the further development of their applications. To solve these two challenges, we decided to re-examine all factors affecting the efficiency of TAPP synthesis, and herein, we present the results of our study.

RESULTS AND DISCUSSION

While re-examining the large-scale synthesis of TAPPs, the most important factors we took into consideration were reproducibility (in yield, impurity profile, reaction setup, course, and workup) and ease of operation (no chromatography, etc.), which determined the attractiveness of the small-scale method. Also important, but of lower significance, were cost (as necessary reagents are simple, inexpensive aromatic aldehydes and amines, and the reaction is catalyzed by a low-cost transition-metal salt), sourcing, waste handling (our method involves acceptable solvents), and safety (no exotherms, no bad decomposition profiles). Considering these, we analyzed the plausible mechanism of TAPP formation (Scheme 1).^{14a}

Although some aspects of this reaction, including the role of the catalyst, are still not fully understood, the first stage, i.e., Schiff base formation, is definitely the most flexible, as it proceeds in a broad temperature and solvent range. The second stage, involving a Mannich reaction and cyclocondensations,

followed by oxidation with air, offers much less control possibilities and, consequently, is probably much more sensitive to changes in reaction parameters. What we learned from previous optimization processes is that the highest yields are obtained when reactions are carried out in acidic media, preferably in acetic acid, while the addition of toluene as a cosolvent enables bulky, lipophilic starting materials to participate in the reaction, due to much better solubility in the reaction media.

We decided to conduct the optimization of TAPPs' synthesis at a relatively large scale (4 mmol of diacetyl), 4 times larger than for previous optimizations,^{14b,27} to find optimal conditions more adequate for larger scales. Another factor that we decided to keep constant was the reaction setup, and all optimization steps were performed in 25 mL round-bottom flasks equipped with magnetic stirring bars of the same size (length 20 mm). We also decided to carry out the reactions in open flasks because the addition of a condenser would slow down the diffusion of air into the reaction flask. For the optimization studies, we selected the synthesis of TAPP 3 from diacetyl, 4-cyanobenzaldehyde (1) and 4-*tert*-butylaniline (2). Compound 3 is known in the literature and had been prepared with a low 12% yield²⁵ using TsOH as the catalyst.^{14b,26} We repeated this reaction and obtained the product in an 18% yield (Table 1, entry 1). In the second experiment, we applied our recently optimized conditions;²⁷ namely, we changed the catalyst to iron(III) perchlorate hydrate (6 mol %) and the solvent to a toluene/AcOH mixture (1:1 v/v). As expected, after stirring the reactants at 90 °C for 3 h, we witnessed a large 3-fold increase in the reaction yield to 54% (Table 1, entry 2). As suggested by the proposed reaction mechanism (Scheme 1), oxidation takes place in the final stage of the formation of TAPPs. Thus, we examined an effect of the presence of oxygen on the reaction outcome (Table 1, entries 3–7). Indeed, the reaction performed in a sealed Schlenk flask under an argon atmosphere with a catalytic amount of iron(III) perchlorate gave product 3 in a 14% yield (Table 1, entry 3). Although the yield is significantly lower, it is not indiscernible, which is reasoned by the oxidative nature of perchlorate. Indeed, in the case of the reaction conducted under an ambient atmosphere with solvents bubbled with argon prior to use, without the addition of any catalyst, the yield dropped even lower to 4% with a noticeably slower reaction rate (Table 1, entry 4). Most likely, a trace amount of the product is formed, due to the presence of the unreacted Schiff base, which also can react as an oxidant. Concurrently, the air atmosphere facilitated the formation of 3 in a 12% yield (Table 1, entry 5). These results show a significant role of oxygen as well as a complexity of the multicomponent reaction mechanism. On the other hand, under pure oxygen gas, the reaction yield was comparable to that of the experiment under air as an oxygen source (Table 1, entry 6). In addition, the reaction rate under oxygen seemed to be much faster, judged from the speed of color changes of the reaction mixture. However, after the fast formation of a bright yellow suspension of the product, we observed a quick darkening of the reaction mixture, which after 3 h of stirring appeared almost black, whereas under air at this point, the reaction mixture was still a brownish-orange suspension. This suggested that pure oxygen is too aggressive and may have caused further oxidation of the formed TAPP to some dark decomposition products. Hence, we shortened the reaction time to 0.5 h but the yield was not improved (Table 1, entry 7). Therefore, it can be concluded that for the synthesis of TAPP, air is a more optimal oxygen source than pure oxygen gas, owing to the reduced risk of

Scheme 1. Simplified, Plausible Mechanism of Multicomponent Reaction Leading to TAPPs

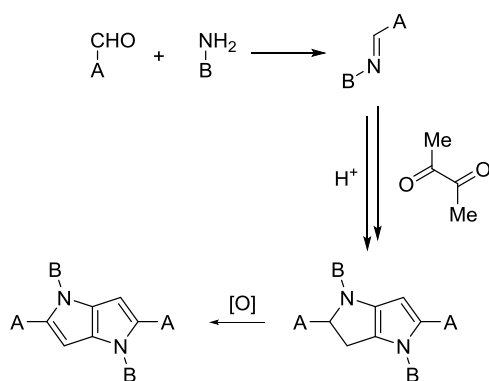
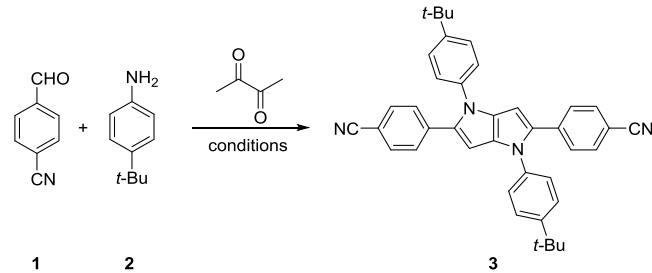


Table 1. Optimization Experiments Using 4-Cyanobenzaldehyde (1, 8 mmol), 4-*tert*-Butylaniline (2, 8 mmol), and Diacetyl (4 mmol)


entry	catalyst (mol %)	solvent (mL/mL)	temp. (°C)	time (h)	oxidant	yield (%)
1	TsOH (10)	AcOH (8)	90	3	air	18
2	Fe(ClO ₄) ₃ ·H ₂ O (6)	AcOH/toluene (6/6)	90	3	air	54
3	Fe(ClO ₄) ₃ ·H ₂ O (6)	AcOH/toluene (6/6)	90	3	^a	14
4	—	AcOH/toluene (6/6)	50	16	^a	4
5	—	AcOH/toluene (6/6)	50	16	air	12
6	Fe(ClO ₄) ₃ ·H ₂ O (6)	AcOH/toluene (6/6)	90	3	O ₂	56
7	Fe(ClO ₄) ₃ ·H ₂ O (6)	AcOH/toluene (6/6)	90	0.5	O ₂	45
8	Fe(ClO ₄) ₃ ·H ₂ O (6)	AcOH/toluene (6/6)	50	16	air	69
9	Fe(ClO ₄) ₃ ·H ₂ O (6)	AcOH/toluene (6/6)	50	16	air ^b	69
10	Fe(ClO ₄) ₃ ·H ₂ O (6)	AcOH/toluene (6/6)	50	16	air ^c	24
11	Fe(ClO ₄) ₃ ·H ₂ O (6)	AcOH/toluene (8/8)	50	16	air	67
12	Fe(ClO ₄) ₃ ·H ₂ O (6)	AcOH/toluene (6/6)	rt	16	air	46
13	Fe(ClO ₄) ₃ ·H ₂ O (6)	AcOH/toluene (6/6)	rt	16	O ₂	37
14	Fe(ClO ₄) ₃ ·H ₂ O (6)	AcOH/toluene (6/6)	50	3	O ₂	67
15	Fe(ClO ₄) ₃ ·H ₂ O (10)	AcOH/toluene (6/6)	50	16	air	69
16	Fe(ClO ₄) ₃ ·H ₂ O (2)	AcOH/toluene (6/6)	50	16	air	50
17	Fe(ClO ₄) ₃ ·H ₂ O (6)	AcOH/toluene (6/6)	35	64	air	65
18	Fe(ClO ₄) ₃ ·H ₂ O (6) ^d	AcOH/toluene (3/3)	50	16	air	65
19	Fe ₂ O ₃ (6) ^d	AcOH/toluene (3/3)	50	16	air	13
20	Fe ₂ (SO ₄) ₃ ·H ₂ O (6) ^d	AcOH/toluene (3/3)	50	16	air	21
21	FeCl ₃ (6) ^d	AcOH/toluene (3/3)	50	16	air	21
22	Fe(OTf) ₃ (6) ^d	AcOH/toluene (3/3)	50	16	air	64
23	Fe(OTf) ₂ (6) ^d	AcOH/toluene (3/3)	50	16	air	51
24	Fe(OAc) ₂ (6) ^d	AcOH/toluene (3/3)	50	16	air	22
25	Fe(OTs) ₃ ·6H ₂ O (6) ^d	AcOH/toluene (3/3)	50	16	air	63
26	Fe(acac) ₃ (6) ^d	AcOH/toluene (3/3)	50	16	air	47
27	HClO ₄ (10)	AcOH/toluene (6/6)	50	16	air	48
28	VO(acac) ₂ (6)	AcOH/toluene (6/6)	50	16	air	15
29	CeF ₄ (6)	AcOH/toluene (6/6)	50	16	air	13
30	NbCl ₅ (6)	AcOH/toluene (6/6)	50	16	air	48
31	Mn(OTf) ₂ (6)	AcOH/toluene (6/6)	90	3	air	38
32	Fe(ClO ₄) ₃ ·H ₂ O (3)	AcOH/toluene (6/6)	90	3	air	43
	Cu(OAc) ₂ (3)					

^aReaction conducted under an argon atmosphere. ^bReaction conducted under a constant air flow (rate: 4 mL/min). ^cReaction conducted under a constant air flow (rate: 60 mL/min). ^dTwice smaller reaction scale, 2 mmol of diacetyl.

overoxidation of sensitive products and ease of operation, not to mention safety matters. Having this established, wanting to keep other parameters unchanged, we then decided to focus mostly on reaction temperature and time. Our analysis of this problem led us to propose that one of the key factors in the synthesis of TAPPs is the accessibility of oxygen. It can be easily estimated that to form 4.0 mmol of the product, roughly 96 mL of pure oxygen gas or over 450 mL of air (under normal conditions) is required. While at small-scale reactions this factor is negligible, scaling up the process may lead to decreased and inefficient access to oxygen and a potential drop in the reaction yields, as a consequence of the square-cube law. Hence, to ensure good contact between the reactants and oxygen, in the next optimization steps, we decided to perform the reactions at

lower temperatures and for longer times. We reasoned that lowering the temperature should lead to increased solubility of oxygen gas in the reaction system. Moreover, the lower temperature should also prevent a potential loss of diacetyl via evaporation (boiling point of 88 °C). In our previous studies, it turned out that this reaction occurs even at room temperature, although it is heterogeneous and the obtained yields are slightly lower. We expected that it could cause some problems with less soluble substrates; therefore, we decided to set up the reaction at 50 °C for 16 h. To our delight, under these conditions, the reaction of 4-*tert*-butylaniline with 4-cyanobenzaldehyde and diacetyl in a 2:2:1 molar ratio in the presence of 6 mol % iron(III) perchlorate hydrate as the catalyst in a mixture of toluene and acetic acid (1:1 v/v) as solvent provided the desired

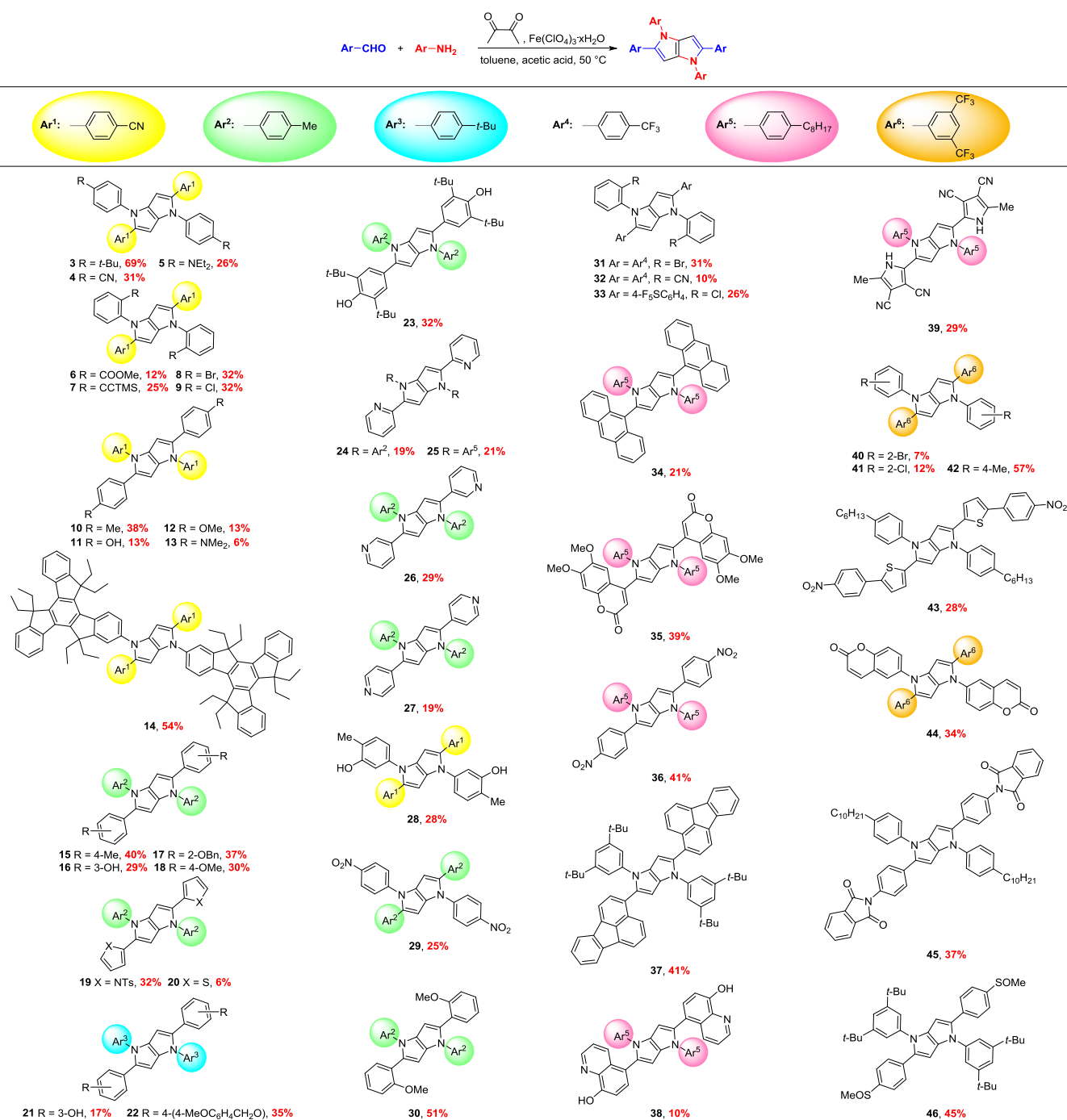


Figure 1. Synthesis of TAPPs—substrate scope including challenging amines and aldehydes.

TAPP 3 in a 69% yield (Table 1, entry 8). It is worth mentioning that we tested the difference between dynamic and static air atmospheres (Table 1, entries 9 and 10). Product 3 was obtained in exactly the same yield (69%) under a constant air stream with a flow rate of 4 mL/min. Increasing the flow rate to 60 mL/min led to a noticeable drop of yield to 24%, due to evaporation of solvents. Dilution of the reaction mixture did not improve the yield (Table 1, entry 11), and a further decrease of the temperature to ambient conditions led to a significant drop in the reaction yields (entries 12 and 13). A good yield of TAPP 3 (65%) could still be obtained even at 35 °C, but the reaction time had to be elongated to 64 h (entry 17). Interestingly, at 50 °C, the reaction could be shortened to 3 h when pure oxygen was

used as an oxidant without appreciable loss in efficiency (Table 1, entry 14). A catalyst loading of 6 mol % seems to be optimal since the increase of this amount to 10 mol % furnished the product in the same yield (69%, Table 1, entry 15), and the decrease to 2 mol % caused a drop in the reaction yield to 50% (Table 1, entry 16). We also investigated whether iron(III) perchlorate can be replaced with different iron sources (entries 19–26). The use of iron(III) oxide, iron(III) sulfate hydrate, iron(III) chloride, and iron(II) acetate provided poor yields of the product (13–22%), which in most cases was due to low solubility of these iron compounds in the reaction medium. Better results were obtained using iron(II) trifluoromethanesulfonate and iron(III) acetoacetonate; however, the yields of

≈50% were still considerably lower than with iron(III) perchlorate under the same conditions. Iron(III) trifluoromethanesulfonate and iron(III) *p*-toluenesulfonate hexahydrate proved almost as efficient as the perchlorate, leading to isolated yields of 64 and 63%, respectively. While due to much higher prices of these two reagents, iron(III) perchlorate still remains an optimal catalyst, they may be convenient replacements, e.g., for industrial-scale reactions where using large amounts of perchlorates may pose considerable safety hazards. Generally, iron(III) salts proved more effective catalysts than iron(II) salts. Furthermore, an experiment with the catalytic amount of perchloric acid gave **3** in a 48% yield (Table 1, entry 27), higher than the reaction without any catalyst and lower than the reaction with iron(III) perchlorate, indicating the importance of both cation and anion on the catalyst performance. Replacing the catalyst with VO(acac)₂, cerium(IV) fluoride, niobium(V) chloride, manganese(II) triflate, or addition of copper(II) salts did not improve the yields (Table 1, entries 28–32). The choice of catalysts was based on the assumption that an oxidant that was also a Lewis acid may facilitate the final oxidation step. It is worthwhile to add that in our hands NbCl₅ is not an efficient catalyst for TAPP formation under the originally published reaction conditions, i.e., in CH₃CN.²⁸

To probe the synthetic utility of the optimized reaction setup (first step: toluene/AcOH = 1:1, 1 h, 50 °C; second step: toluene/AcOH = 1:1, Fe(ClO₄)₃·H₂O, 16 h, 50 °C) (Table 1, entry 8), we subjected a range of sterically hindered and electronically diverse aldehydes and primary aromatic amines to these conditions, attempting to both increase the reaction scope and investigate if larger scale will deliver pure TAPPs in nondiminished yields (Figure 1).

The above-discussed modified method gives equal or higher yields of TAPPs than those previously reported for almost all substituted benzaldehydes and anilines trialed. Typically, pyrrolo[3,2-*b*]pyrroles are obtained in good yields from electron-poor aldehydes (TAPPs **3–5**, **7–9**, **14**, **36**, **42**, and **46**; Figure 1). Importantly, lowering the reaction temperature allowed for the first time the use of electron-rich aldehydes; however, the obtained yields were reduced (TAPPs **11–13**, **16**, **19**, **23**, and **38**; Figure 1). The most outstanding expansion of scope is TAPPs synthesized from sterically hindered primary aromatic amines. The attempts to prepare TAPPs from 2-chloroaniline or 2-bromoaniline under previously developed conditions^{14a,b} gave yields below the detection limit. Under the new conditions, anilines with halo-, carboxy-, cyano-, or even (trimethylsilyl)ethynyl substituents in the ortho position now lead to the corresponding TAPPs **6**, **7**, **8**, **9**, **31**, **32**, **33**, **40**, and **41** (Figure 1) in up to 32% yield, opening the door for their further functionalization. Exceptionally sterically hindered amines, for example, 2,4,6-trimethylaniline, do not participate in this reaction; however, TAPP **34** bearing bulky 9-anthracenyl groups was obtained with acceptable yield from the corresponding anthracene-9-carboxaldehyde. In addition, pyrrolo[3,2-*b*]pyrroles decorated with other polycyclic aromatic hydrocarbons, fluoranthene and truxene (TAPPs **37** and **14**, respectively), could be obtained in surprisingly good yields, giving the possibility for significant expansion of the pyrrolo[3,2-*b*]pyrrole π -electron system. This result may prove particularly important since the combination of electron-rich pyrrolo[3,2-*b*]pyrrole core with extended π -electron substituents makes the discussed systems potentially hole-transporting materials.

Another valuable result is the possibility of transforming various heterocycle-derived aldehydes, both 5-membered

heterocyclic aldehydes and 6-membered pyridine derivatives, into the corresponding products **19**, **20**, **24–27**, **39**, and **43** (Figure 1). These conditions also turned out to be effective for the synthesis of TAPPs from substituted 2-formylpyrrole and 2-formylthiophene.

Nevertheless, not all aromatic amines can form TAPPs. For example, the reaction of 4-cyanobenzaldehyde with 3-aminophenol or 3-aminoanisole did not lead to the desired product. Interestingly, 4-amino-2-hydroxytoluene, which contains a *para*-substituent, gave TAPP **28** under the same conditions.

In addition, we enriched the library of substrates with a set of hydroxybenzaldehydes, which under developed conditions afforded the corresponding products with moderate yields (TAPPs **11**, **16**, **21**, **23**, and **38**; Figure 1). For these substrates, the best outcomes (up to 32%, TAPPs **16** and **23**) were obtained for TAPPs bearing an electron-donating substituent on the *N*-aryl ring, while 4-cyanoaniline afforded the corresponding dye **11** in only a 13% yield. Alternatively, hydroxyphenyl-substituted pyrrolopyrroles are achievable via *O*-benzyl or *O*-(4-methoxybenzyl)-protected derivatives (TAPPs **17** and **22**, respectively), which are available in good yields and can in principle be deprotected using known methods. Moreover, TAPP **45** possessing a phthalimide moiety can be also synthesized. One of the biggest breakthroughs was achieved with coumarins, bearing formyl or amino groups in various positions. The success of this attempt was not obvious, as various side reactions could be expected, including the Lewis acid-catalyzed Michael addition of pyrrolopyrrole and coumarin scaffolds. Indeed, early attempts of TAPP preparation from formyl-coumarins and amino-coumarins with TsOH as the catalyst failed. The first member of the coumarin-TAPP family, compound **35**, was obtained in a fairly good 39% yield, which prompted us to test other coumarin derivatives as starting materials, and we found that coumarins can be used as both amine (as 6-amino-coumarin) and aldehyde components in the TAPP preparation. The resulting compound **44** was obtained in a 34% yield. It is noteworthy that TAPP **35** (Figure 1) is the first pyrrolo[3,2-*b*]pyrrole to date prepared from an aldehyde bearing CHO attached to the carbon-carbon double bond rather than to the aromatic ring.

With these results in hand, we attempted the large-scale synthesis of TAPPs. Aiming to keep the reaction setup and workup as simple as possible, we tested this methodology with selected amines, aldehydes, and diacetyl used in amounts of 80:80:40 mmol, with the reaction carried out in an open three-neck flask (to facilitate access to air; see the Supporting Information (SI) for further information). To our delight, the reaction was fully reproducible at large scale, giving products **3**, **9**, **15**, and **24**, with high purity and with virtually the same yield as in smaller-scale experiments, with all of the advantages of the latter, namely, simplicity of the reaction setup and workup (Figure 2).

To demonstrate the synthetic potential of the newly developed method, we decided to use 1,4-dihydro-pyrrolo[3,2-*b*]pyrrole obtained from 2-haloanilines in the preparation of heteroanalogues of polycyclic aromatic hydrocarbons (PAHs). Therefore, we obtained the dibromo-TAPP **49**, which was subsequently transformed into the fused derivative **50** by palladium-catalyzed direct arylation (Scheme 2). Its structure was unambiguously confirmed by X-ray analysis (see the SI for further details; Figure S2). We recently described the synthesis of heterocycles possessing this skeleton either by direct arylation with TAPP obtained from *ortho*-bromo-substituted

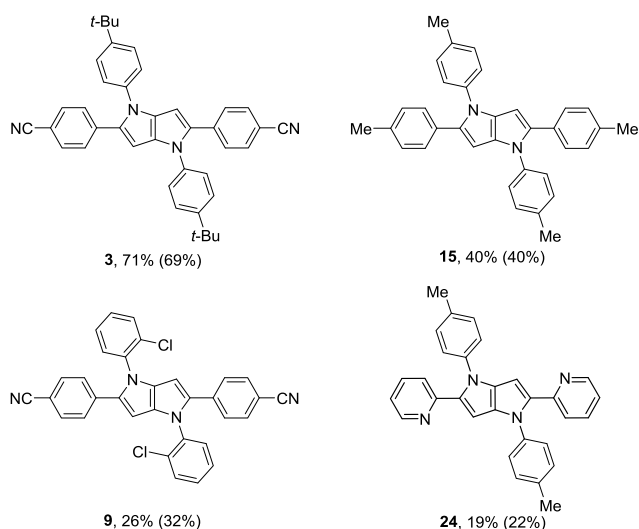
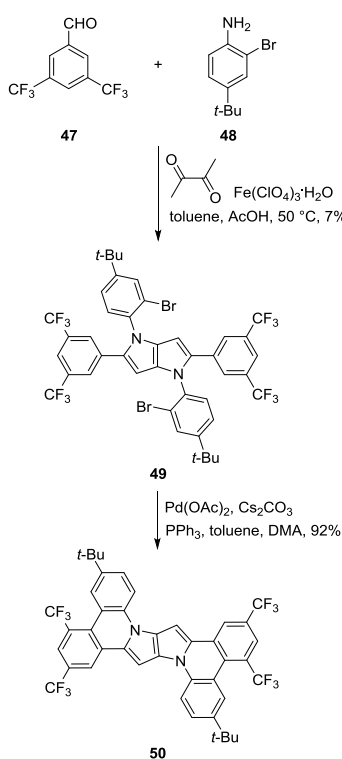


Figure 2. Large-scale (200 mmol, sum of all starting materials) preparation of TAPPs. The yield obtained in a 20 mmol experiment is given in parentheses.

Scheme 2. Preparation of π -Expanded TAPP 50

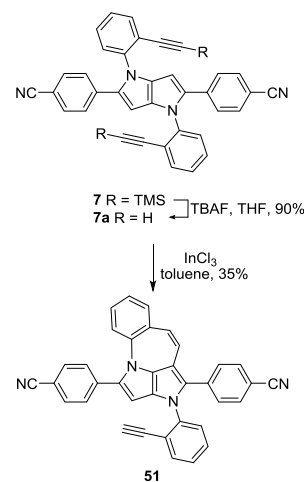


benzaldehydes^{13d} or by 1,2-aryl shift in tetraarylpyrrolo[3,2-*b*]pyrroles.²⁹ The present approach is an alternative route giving easy access to quite elaborated hetero-PAHs in just a two-step synthesis. Interestingly, the double intramolecular direct arylation proceeds regioselectivity at phenyl rings adjacent to positions 2 and 5. This underlines the strong influence of the pyrrolo[3,2-*b*]pyrrole core, which markedly increases the electron density on these substituents affecting their reactivity.

Aiming to further execute the advantages of this method, we took into consideration the annulation leading to π -expanded TAPPs. Such a strategy requires TAPPs decorated with a carbon–carbon triple bond located on the *N*-aryl ring and

should afford a dye with improved conjugation between the core and substituents originating from parent aniline. Thus, we transformed parent pyrrolo[3,2-*b*]pyrrole 7a (Scheme 3) in the

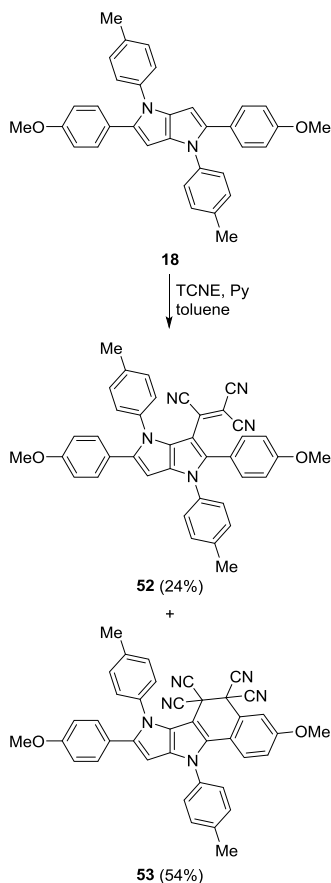
Scheme 3. Synthesis of Dye 51 Possessing a Seven-Membered Ring



presence of indium(III) chloride³⁰ into the fused analogue. The reaction leads predominantly to 7-endo-dig cyclization product 51, which was only isolated in a 35% yield due to limited stability. The preference for the 7-endo-dig pathway versus 6-exo-dig pathway seems to be related to both the nature of the catalyst and the structure of the substrate, which makes the formation of a seven-membered ring possible. It is likely, however, that the product containing a new six-membered ring forms albeit due to its reactivity, it reacts further under the reaction conditions. The plausible rationale behind the fact that the second annulation did not occur is the strong altering of electron distribution in molecule 51 compared to that in TAPP 50. A thorough analysis of one-dimensional (1D) NMR and two-dimensional (2D) NMR spectra provides sufficient structural information about compound 51. ¹H NMR spectra show two singlets, originating from the core proton (6.22 ppm) and ethynyl proton (3.15 ppm), as well as two AA'XX' systems (from substituents at positions 2 and 5). Such observations indicate the desymmetrization of the structure caused by monoannulation. Moreover, the number of correlations at ¹H¹³C HSQC spectra, which is equal to the number of magnetically nonequivalent protons, can be rationalized only by the formation of the 7-endo-dig product (Figure S1) and excludes the 6-egzo-dig regioisomer. A thorough analysis of NOESY, ¹H¹³C HSQC, and ¹³C¹³C HMBC spectra finally uncovers the structure of 51, supporting previous considerations. The formation of seven-membered rings was heretofore unreported for alkyne benzannulation.³⁰

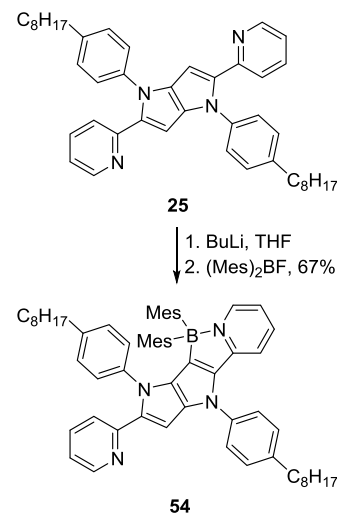
As we mentioned in our previous papers, the extremely electron-rich character of the pyrrolo[3,2-*b*]pyrrole scaffold is sometimes manifested by its unexpected reactivity.^{29,31} In Scheme 4, we show another example of such a phenomenon. Looking for TAPPs with strongly polarized structures, we attempted the reaction of TAPP 18 with tetracyanoethylene (TCNE) in boiling toluene in the presence of pyridine,^{32a} which in line with our expectation resulted in the formation of compound 52, however, only in a relatively small yield. To our surprise, the main product formed during this reaction was compound 53, apparently being a result of a tandem Diels–

Scheme 4. Reaction of TAPP 18 with Tetracyanoethylene



Alder/reoxidation reaction. Its structure was unambiguously confirmed by NMR, MS, and X-ray analysis (see the SI for further details; Figure S3). Although the chemistry of TCNE is very rich,^{32b,c} to the best of our knowledge, this is the only example of biphenyl (or heteroaryl-phenyl derivative) participating in such a transformation and, in general, a rare example of the Diels–Alder reaction taking place on a nonactivated benzene ring. It is worth pointing out that the presence of pyridine is crucial for this reaction, and despite the presence of an excess of TCNE, only monosubstitution was achieved. Moreover, TAPP 3 bearing electron-withdrawing substituents does not undergo this process, which underlines again the relatively strong coupling of aryl rings at positions 2 and 5 with pyrrolo[3,2-*b*]pyrrole core.

Finally, an easy access to 2-pyridine-substituted TAPPs prompted us to use them for the synthesis of *N,C*-chelated boron compounds (Scheme 5). In the past decade, 2-phenylpyridine-derived four-coordinate organoboron chelates have been extensively studied, mostly by the group of Wang, and found to show interesting properties, including photochromic reactivity,³³ two-photon absorption,³⁴ strong emission, high photostability,³⁵ etc. Following the well-established protocol, we treated compound 25 with BuLi, and the resulting lithiated intermediate was reacted with dimesitylboron fluoride, which yielded compound 54 (Scheme 5). Bis-substitution was not achieved despite numerous trials, probably due to the problem with bis-lithiation, which might be hampered due to the unfavorable electrostatic interaction within the pyrrolopyrrole core.

Scheme 5. Synthesis of *N,C*-Chelated Boron TAPP 54

Having synthesized a library of new dyes, we investigated their fundamental photophysical properties. All measurements were performed in toluene as a solvent. Generally, unless decorated with strongly electron-withdrawing or electron-donating substituents at positions 2 and 5 of the central core, pyrrolopyrroles exhibit a broad, featureless absorption band at 350–375 nm with molar extinction coefficients (ϵ) of 10 000–40 000 M⁻¹ cm⁻¹ and emission maxima located at 400–420 nm with fluorescence quantum yields (Φ_f) typically ranging from 0.30 to 0.70 (Table 2, Figures 3 and 4). Absorption and emission maxima are red-shifted to 400–410 and 450–460 nm, respectively, for compounds 3–9 bearing electron-withdrawing 4-cyanophenyl residues at positions 2 and 5. At the same time, these compounds exhibit higher ϵ values of 40 000–60 000 M⁻¹ cm⁻¹ with larger $\Phi_f = 0.50$ –0.90. Placing sterically hindered substituents at positions 1 and 4 does not influence the absorption and emission maxima underlying the relatively weak electronic coupling on *N*-substituents with the heterocyclic core. The most bathochromically shifted absorption (504 nm) and emission (647 nm) maxima among the synthesized dyes were exhibited by TAPP 43 bearing nitrophenyl substituents attached to the pyrrolopyrrole core through the thiophene linker (Figure 3). The remarkable red shift of both absorption and emission spectra is attributed to two factors, i.e., (1) extremely strong electron-withdrawing character of nitrophenyl substituents and (2) smaller dihedral angle between aryl substituents and the pyrrolo[3,2-*b*]pyrrole core (effect of the five-membered ring)²⁷ leading to more effective π -conjugation. Conversely, substitution of the pyrrolo[3,2-*b*]pyrrole core with strong electron-donating groups at positions 2 and 5 (dyes 11–13 and 19) leads to only a slight red shift of absorption (349–395 nm), whereas a prominent red shift of emission (446–534 nm) resulting in large Stokes' shifts of 6200–8300 cm⁻¹ suggests a notable difference in geometry of the S₁ excited state and S₀ ground state. The concomitant drop in fluorescence intensities ($\Phi_f = 0.04$ –0.08) is likely due to the occurrence of charge-transfer processes.

As thoroughly discussed earlier,¹³ substituents located at positions 2 and 5 of pyrrolo[3,2-*b*]pyrrole scaffold have a significantly stronger impact on the optical features compared with those located at positions 1 and 4 (attached to nitrogen atoms). This is clearly manifested in the series of dyes 6–9 and 14 possessing sterically congested 2-halophenyl- or 2-carboxyphenyl- and truxene subunits attached to nitrogen atoms.

Table 2. Spectroscopic Properties of New TAPPs Measured in Toluene

comp.	$\lambda_{\text{abs}}^{\text{max}}$ (nm)	$\epsilon \cdot 10^{-3}$ ($\text{M}^{-1} \cdot \text{cm}^{-1}$)	$\lambda_{\text{em}}^{\text{max}}$ (nm)	Stokes shift (cm^{-1})	Φ_{fl}
3	403	53	450	2600	0.76 ^a
5	413	57	460	2500	0.76 ^b
6	407	47	454	2600	0.15 ^b
7	413	60	447	1800	0.90 ^b
8	403	55	443	2200	0.46 ^b
9	402	50	443	2300	0.86 ^b
10	321	56	470	5400	0.14 ^b
11	322; 370	61; 11	533	8300	0.05 ^b
12	321; 368	58; 12	496	7000	0.08 ^b
13	326; 395	50; 11	548	7000	0.04 ^b
14	402	48	451	2700	0.93 ^b
15	352	23	408	3900	0.66 ^a
16	355	34	409	3700	0.57 ^a
17	348	27	414	4600	0.50 ^a
18	348	n.d.	412	4500	0.52 ^a
19	300; 350	50	446	6200	0.08 ^b
21	356	24	410	3700	0.77 ^b
22	350	37	414	4400	0.59 ^a
23	355	29	413	4000	0.88 ^a
24	379	43	416	2400	0.82 ^b
25	377	46	419	2700	0.66 ^a
28	407	52	452	2400	0.35 ^b
31	375	38	415	2600	0.27 ^b
32	367	35	443	4700	0.09 ^a
33	380	45	421	2600	0.32 ^b
35	370	32	462	5400	0.54 ^b
38	402	12			
39	370	30	448	4700	0.80 ^a
40	377	40	416	2500	0.18 ^b
41	376	41	416	2600	0.48 ^b
42	380	37	417	2300	0.57 ^b
43	504	44	645	4400	0.41 ^c
44	370	38	419	3200	0.08 ^b
45	376	51	421	2800	0.0004 ^b
46	375	40	431	3500	0.83 ^b
49	379	42	417	2400	0.19 ^b
50	370	34	575	6300	0.05 ^b
	419	27			
	442	25			
51	408	37	526	5500	0.34 ^b
52	327; 476; 605	35; 7; 3	433	7500	0.001 ^a
53	395	27			
54	374; 451	33; 23	534	3400	0.54 ^d

^aFluorescence quantum yield determined with quinine sulfate as a reference. ^bFluorescence quantum yield determined with 9,10-diphenylanthracene as a reference. ^cFluorescence quantum yield determined with fluorescein as a reference. ^dFluorescence quantum yield determined with coumarin 153 as a reference.

Undoubtedly, steric factors impose larger dihedral angles between *N*-aryl substituents and the central core, causing breakage of electronic communication between them. Nevertheless, the effect on both absorption and emission spectra is negligible in regard to sterically unencumbered **3**, indicating a minor contribution of amine-originating substituents on the overall optical characteristics. As far as **14** is concerned, a deeper comparative analysis of absorption spectra indicates a clear increase of the molar absorption coefficient in the high-energy

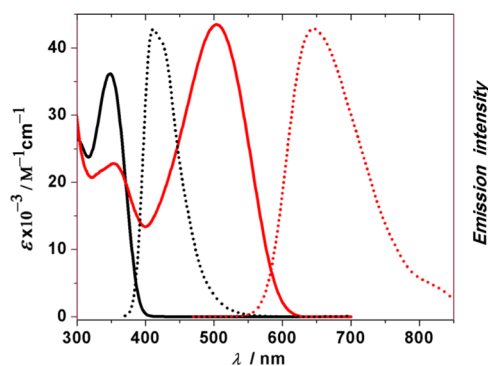


Figure 3. Absorption (solid line) and normalized emission (dotted line) spectra of **18** (black) (excitation at 350 nm) and **43** (red) (excitation at 460 nm) measured in toluene at concentrations of 3.53 μM for **18** and 4.26 μM for **43**. Emission intensity is given in arbitrary units.

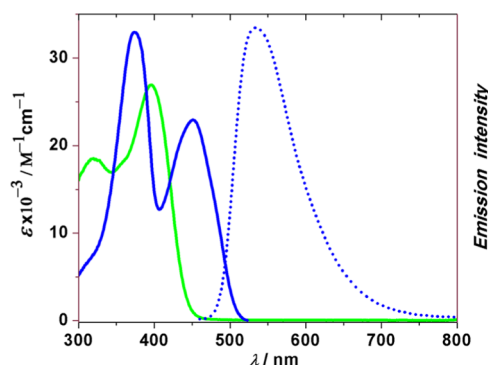


Figure 4. Absorption (solid line) and normalized emission (dotted line) spectra of **53** (green) and **54** (blue) (excitation at 450 nm) measured in toluene at concentrations of 3.44 μM for **53** and 3.40 μM for **54**. Emission intensity is given in arbitrary units.

part of the spectrum, which is most likely caused by the presence of the truxene subunit. Of particular note is the strong blue fluorescence (Φ_{fl} reaching 0.93). One of the factors responsible for the observed excellent emissive properties could be symmetry-breaking within the truxene core.³⁶

The new methodology allowed for the first time synthesis of coumarin-containing pyrrolopyrrole dyes **35** and **44**. Their spectral features differ markedly, depending on the substitution pattern, giving the opportunity for fine-tuning the desired properties. In the case of TAPP **44**, the fluorescence quantum yield is low, which is in agreement with the general trend observed for coumarins possessing electron-donating substituents at position 6.³⁷ The bulky coumarin-4-yl substituent present at positions 2 and 5 of TAPP **35** results in the large difference in dihedral angles between ground- and excited-state geometries, which in turn manifests in the large Stokes shift. According to expectations, the π -extension of fused analogue **50** leads to a significant bathochromic shift of the absorption (442 nm) and emission (575 nm) maxima. In the absorption spectrum, two main bands with fine-vibronic features located at 370 and 420–440 nm are present, which is attributed to the rigidity of the structure. Surprisingly, a significant decrease of the fluorescent quantum yield is observed, most likely due to predominant radiationless de-excitation. We observed a similar tendency for the annulated dye **51**, which shows a decreased fluorescence response when compared to that for the parent TAPP **7**. Moreover, as for TAPP **50**, the formation of a seven-

membered ring strongly shifts both absorption and emission maxima; however, for compound **51**, it is in the opposite direction (hypsochromically λ_{abs} and bathochromically λ_{em}), which results in a large Stokes' shift of 5500 cm^{-1} .

CONCLUSIONS

Lowering the reaction temperature to $50 \text{ }^\circ\text{C}$ enabled more control of the course of the multicomponent reaction leading to tetraarylpyrrolo[3,2-*b*]pyrroles. This makes it possible to maintain high yields when increasing the scale to 4.0 and even 40 mmol. Simultaneously, the electron-rich aldehydes and sterically hindered anilines become compatible with this reaction and numerous corresponding TAPPs are obtained. Our findings expand the spectrum of possible tetraarylpyrrolo[3,2-*b*]pyrroles that can be prepared. These new reaction conditions proved to be extremely efficient in the synthesis of potentially useful halogen derivatives of pyrrolo[3,2-*b*]pyrroles, which was demonstrated by the synthesis of heteroanalogues of polycyclic aromatic hydrocarbons. The exceptionally high-lying highest occupied molecular orbital (HOMO) of TAPPs has a profound influence on their reactivity. Indeed, it influences the electron density of the neighboring aryl substituents, which results in (a) preferential direct arylation occurring at positions 2 and 5 activated by pyrrolo[3,2-*b*]pyrrole core as an electron-donating substituent, (b) spontaneous reaction of TAPP with TCNE including a unique Diels–Alder reaction, and (c) unprecedented alkyne benzannulation with the formation of a seven-membered ring. The possibility to introduce such a broad range of electronically and sterically diverse substituents at positions 1, 2, 4, and 5 combined with the relatively strong coupling through biaryl linkages translates to an ability to modulate emission wavelengths across the entire visible range. The presence of electron-withdrawing moieties at positions 2 and 5 combined with electron-donating *N*-aryls enables us to increase the Stokes shift to $7000\text{--}8000 \text{ cm}^{-1}$. We envisage that the new reactivity reported herein will not only influence directions of the chemistry of aza-nanographenes but also underpin the development of novel optoelectronic materials.

EXPERIMENTAL SECTION

General Information. All chemicals were used as received unless otherwise noted. Reagent-grade solvents (MeCN, CH_2Cl_2 , hexane, toluene) were distilled prior to use. All reported NMR spectra were recorded on a 500 MHz spectrometer unless otherwise noted. Chemical shifts (δ ppm) for ^1H and ^{13}C NMR were determined with TMS as the internal reference; *J* values are given in Hz. UV–vis absorption and emission spectra were recorded in toluene. For all fluorescence measurements, spectrofluorometer slits were set at 2.5 nm. Fluorescence spectra were obtained by excitation at 350 nm for compounds **3**, **15–18**, **22**, **23**, **25**, **32**, **39**, and **52**; 373 nm for compounds **5–14**, **19**, **21**, **24**, **28**, **31**, **33**, **35**, **40–42**, **44–46**, and **49–51**; 450 nm for **54**; and 460 nm for **43**. Chromatography was performed on silica (Kieselgel 60, 200–400 mesh). Mass spectra were obtained with an EI ion source and the EBE double focusing geometry mass analyzer or spectrometer equipped with an electrospray ion source with a quadrupole time-of-flight (q-TOF)-type mass analyzer. The analytical data for compounds **3**, **4**, **15**, **20**, **26**, **27**, **29**, and **34** have been described previously.

Synthesis. General Procedure for the Synthesis of Pyrrolo[3,2-*b*]pyrroles on a 20 mmol (Sum of All Starting Materials) Scale. Glacial acetic acid (6 mL), toluene (6 mL), aldehyde (8 mmol), and aniline (8 mmol) were placed in a 25 mL round-bottom flask equipped with a magnetic stir bar. The mixture was stirred at $50 \text{ }^\circ\text{C}$ for 1 h. After that time, $\text{Fe}(\text{ClO}_4)_3 \cdot x\text{H}_2\text{O}$ (85 mg) was added, followed by diacetyl (0.35 mL, 4 mmol). The resulting mixture was stirred at $50 \text{ }^\circ\text{C}$ (oil

bath) in an open flask under air overnight. The precipitate was filtered off, washed with cold methanol (in some cases, CH_3CN was used), and dried under vacuum. In the event that the product does not precipitate, the organic solvents are removed under reduced pressure, and then the product is obtained by crystallization from acetonitrile. In case the product contains pyridyl or amino substituent, the reaction mixture is quenched with saturated aqueous NaHCO_3 (60 mL). The precipitate was filtered off, washed with H_2O and CH_3CN , and dried under vacuum to afford the pure product.

1,4-Bis(4-(*tert*-butyl)phenyl)-2,5-bis(4-cyanophenyl)-1,4-dihydropyrrolo[3,2-*b*]pyrrole (3). Yellow solid. Yield: 1.58 g (69%). Spectral and optical properties concur with literature data.²⁵

1,2,4,5-Tetrakis(4-cyanophenyl)-1,4-dihydropyrrolo[3,2-*b*]pyrrole (4). Yellow solid. Yield: 0.63 g (31%). Spectral and optical properties concur with literature data.¹⁶

2,5-Bis(4-cyanophenyl)-1,4-bis(4-(diethylamine)phenyl)-1,4-dihydropyrrolo[3,2-*b*]pyrrole (5). Yellow solid. Yield: 0.64 g (26%). M.p. $309\text{--}310 \text{ }^\circ\text{C}$. ^1H NMR (500 MHz, CDCl_3) $\delta = 7.45$ (d, *J* = 8.4 Hz, 4H), 7.30 (d, *J* = 8.4 Hz, 4H), 7.08 (d, *J* = 8.8 Hz, 4H), 6.66 (d, *J* = 8.9 Hz, 4H), 6.40 (s, 2H), 3.39 (q, *J* = 7.0 Hz, 8H), 1.20 (t, *J* = 7.0 Hz, 12H) ppm; ^{13}C { ^1H } NMR (126 MHz, CDCl_3) $\delta = 146.6$, 138.1, 135.0, 133.8, 131.8, 127.6, 127.5, 126.7, 119.4, 112.0, 108.4, 94.6, 44.4, 12.6 ppm. HRMS (EI): *m/z* calcd for $\text{C}_{40}\text{H}_{38}\text{N}_6$: 602.3158 [M^+]; found: 602.3174.

2,5-Bis(4-cyanophenyl)-1,4-bis(2-(methoxycarbonyl)phenyl)-1,4-dihydropyrrolo[3,2-*b*]pyrrole (6). Yellow solid. Yield: 0.27 g (12%). M.p. $275\text{--}276 \text{ }^\circ\text{C}$. ^1H NMR (500 MHz, CDCl_3 , mixture of atropoisomers), $\delta = 7.94\text{--}7.84$ (m, 2H), 7.61–7.54 (m, 2H), 7.50–7.44 (m, 2H), 7.42 (d, *J* = 8.4 Hz, 4H), 7.38 (d, *J* = 7.7 Hz, 1H), 7.32 (d, *J* = 7.5 Hz, 1H), 7.19 (dd, *J* = 8.5, 2.2 Hz, 4H), 6.32 (s, 1H), 6.30 (s, 1H), 3.59 (s, 6H) ppm; ^{13}C { ^1H } NMR (126 MHz, CDCl_3) $\delta = 166.5$, 166.3, 138.8, 138.6, 137.2, 137.1, 136.20, 136.18, 133.8, 133.7, 132.9, 132.8, 132.00, 131.98, 131.3, 131.2, 129.2, 129.0, 128.8, 128.7, 128.6, 128.2, 127.7, 127.53, 127.51, 127.49, 125.3, 119.06, 119.03, 109.14, 109.05, 95.4, 95.0, 52.4 ppm. HRMS (EI): *m/z* calcd for $\text{C}_{36}\text{H}_{24}\text{N}_4\text{O}_4$: 576.1798 [M^+]; found: 576.1784.

2,5-Bis(4-cyanophenyl)-1,4-bis(2-trimethylsilylethylphenyl)-1,4-dihydropyrrolo[3,2-*b*]pyrrole (7). Yellow solid. Yield: 0.16 g (25%). M.p. $271\text{--}272 \text{ }^\circ\text{C}$. ^1H NMR (500 MHz, CDCl_3 , mixture of atropoisomers) $\delta = 7.66$ (dd, *J* = 7.7, 1.4 Hz, 1H), 7.61–7.59 (m, 1H), 7.43 (t, *J* = 8.5 Hz, 4H), 7.37–7.22 (m, 4H), 7.19 (dd, *J* = 8.5, 3.0 Hz, 4H), 7.16 (dd, *J* = 6.0, 3.1 Hz, 1H), 6.94 (d, *J* = 7.1 Hz, 1H), 6.51 (s, 1H), 6.41 (s, 1H), -0.01 (s, 9H), -0.08 (s, 9H) ppm. ^{13}C { ^1H } NMR (126 MHz, CDCl_3) $\delta = 141.6$, 141.1, 138.0, 137.9, 135.7, 135.4, 134.1, 133.7, 133.6, 133.50, 132.0, 131.9, 129.4, 129.2, 128.2, 128.0, 127.1, 127.4, 127.0, 121.4, 120.2, 119.2, 108.7, 108.6, 101.4, 101.3, 101.1, 100.7, 98.69, 96.68, 77.2, 77.0, 76.7, -0.5 ppm. HRMS (EI): *m/z* calcd for $\text{C}_{42}\text{H}_{36}\text{N}_4\text{Si}_2$: 652.2479 [M^+]; found: 652.2471.

2,5-Bis(4-cyanophenyl)-1,4-bis(2-ethylenylphenyl)-1,4-dihydropyrrolo[3,2-*b*]pyrrole (7a). Parent pyrrolo[3,2-*b*]pyrrole **7** (81.3 mg, 0.13 mmol) was dissolved in 2 mL of tetrahydrofuran (THF). Next, tetra-*n*-butylammonium fluoride (TBAF, 1 M solution in THF, 0.35 mL) was added and the resulted mixture was allowed to react at room temperature for 2 h. Subsequently, the solvent was evaporated and the resulted residue was filtered through the silica pad (with dichloromethane (DCM) as the eluent) and crystallized from DCM/hexanes to afford the desired product as a yellow solid 57.5 mg (90%).

Yellow solid. Yield: 57.5 mg (90%). M.p. $274\text{--}275 \text{ }^\circ\text{C}$. ^1H NMR (500 MHz, CDCl_3 , mixture of atropoisomers) $\delta = 7.69\text{--}7.63$ (m, 2H), 7.44–7.34 (m, 9H), 7.25–7.21 (m, 4H), 7.10 (dd, *J* = 5.7, 3.5 Hz, 1H), 6.45 (s, 1H), 6.44 (s, 1H), 3.08 (s, 1H), 3.04 (s, 1H) ppm. ^{13}C { ^1H } NMR (126 MHz, CDCl_3) $\delta = 141.6$, 141.5, 137.9, 137.8, 136.5, 136.4, 134.5, 134.4, 134.1, 133.8, 132.0, 129.9, 129.8, 128.2, 128.1, 127.5, 127.4, 127.3, 120.1, 119.2, 119.1, 110.0, 108.9, 97.1, 96.7, 83.0, 82.8, 80.0, 79.9, 29.7 ppm. HRMS (EI): *m/z* calcd for $\text{C}_{36}\text{H}_{20}\text{N}_4$: 508.1688 [M^+]; found: 508.1678.

1,4-Bis(2-bromophenyl)-2,5-bis(4-cyanophenyl)-1,4-dihydropyrrolo[3,2-*b*]pyrrole (8). Yellow solid. Yield: 0.79 g (32%). M.p. $345\text{--}346 \text{ }^\circ\text{C}$. ^1H NMR (500 MHz, CDCl_3 , mixture of atropoisomers) $\delta = 7.80\text{--}7.72$ (m, 2H), 7.43 (d, *J* = 8.4 Hz, 4H),

7.39–7.29 (m, 5H), 7.19 (m, 5H), 6.39 (s, 1H), 6.38 (s, 1H) ppm. ^{13}C { ^1H } NMR (126 MHz, CDCl_3) δ = 138.9, 137.4, 136.6, 134.1, 134.1, 133.7, 133.5, 132.0, 130.2, 130.1, 129.6, 129.5, 128.6, 128.5, 127.2, 127.1, 121.8, 119.0, 109.1, 96.5, 96.1 ppm. HRMS (EI): m/z calcd for $\text{C}_{32}\text{H}_{18}\text{N}_4\text{Br}_2$: 615.9898 [M^+]; found: 615.9890.

1,4-Bis(2-chlorophenyl)-2,5-bis(4-cyanophenyl)-1,4-dihydropyrrolo[3,2-*b*]pyrrole (9). Yellow solid (poor solubility in common organic solvents). Yield: 0.68 g (32%). M.p. 340–341 °C. ^1H NMR (500 MHz, $\text{DMSO}-d_6$, mixture of atropoisomers) δ = 7.76–7.68 (m, 2H), 7.64 (dd, J = 8.7, 2.3 Hz, 4H), 7.57–7.47 (m, 4H), 7.46–7.40 (m, 1H), 7.37–7.35 (m, 1H), 7.31–7.23 (m, 4H), 6.61 (s, 1H), 6.59 (s, 1H) ppm. HRMS (EI): m/z calcd for $\text{C}_{32}\text{H}_{18}\text{N}_4\text{Cl}_2$: 528.0909 [M^+]; found: 528.0914.

1,4-Bis(4-cyanophenyl)-2,5-bis(4-methylphenyl)-1,4-dihydropyrrolo[3,2-*b*]pyrrole (10). Yellow solid. Yield: 0.74 g (38%). M.p. 330 °C (decomp.). ^1H NMR (500 MHz, CDCl_3) δ = 7.63 (d, J = 8.6 Hz, 4H), 7.34 (d, J = 8.6 Hz, 4H), 7.04–7.13 (m, 8H), 6.42 (s, 2H), 2.35 (s, 6H) ppm; ^{13}C NMR (126 MHz, CDCl_3) δ = 143.6, 137.1, 136.1, 133.2, 130.8, 129.8, 129.3, 128.3, 125.0, 118.6, 108.7, 96.6, 21.2 ppm. HRMS (EI): m/z calcd for $\text{C}_{34}\text{H}_{24}\text{N}_4$: 488.2001 [M^+]; found: 488.2005.

1,4-Bis(4-cyanophenyl)-2,5-bis(4-hydroxyphenyl)-1,4-dihydropyrrolo[3,2-*b*]pyrrole (11). Yellow solid (poor solubility in common organic solvents). Yield: 0.25 g (13%). M.p. 362–363 °C. ^1H NMR (500 MHz, $\text{DMSO}-d_6$) δ 9.53 (s, 2H), 7.85 (d, J = 8.5 Hz, 4H), 7.38 (d, J = 8.5 Hz, 4H), 7.00 (d, J = 8.5 Hz, 4H), 6.70 (d, J = 8.5 Hz, 4H), 6.46 (s, 2H) ppm. ^{13}C { ^1H } NMR (126 MHz, $\text{DMSO}-d_6$) δ 157.0, 143.7, 135.6, 133.9, 130.3, 129.9, 125.3, 123.8, 119.0, 115.9, 110.0, 108.0, 96.8 ppm. HRMS (EI): m/z calcd for $\text{C}_{32}\text{H}_{20}\text{N}_4\text{O}_2$: 492.1586 [M^+]; found: 492.1574.

1,4-Bis(4-cyanophenyl)-2,5-bis(4-methoxyphenyl)-1,4-dihydropyrrolo[3,2-*b*]pyrrole (12). Pale yellow solid. Yield: 0.27 g (13%). M.p. 270 °C (decomp.). ^1H NMR (500 MHz, CDCl_3) δ = 7.63 (d, J = 8.3 Hz, 4H), 7.34 (d, J = 8.2 Hz, 4H), 7.12 (d, J = 8.4 Hz, 4H), 6.83 (d, J = 8.4 Hz, 4H), 6.38 (s, 2H), 3.81 (s, 6H) ppm; ^{13}C { ^1H } NMR (126 MHz, CDCl_3) δ = 158.9, 143.6, 135.6, 133.2, 130.4, 129.7, 125.3, 124.9, 118.6, 114.1, 108.7, 96.3, 55.3 ppm. HRMS (EI): m/z calcd for $\text{C}_{34}\text{H}_{24}\text{N}_4\text{O}_2$: 520.1899 [M^+]; found: 520.1898.

1,4-Bis(4-cyanophenyl)-2,5-bis(4-(dimethylamino)phenyl)-1,4-dihydropyrrolo[3,2-*b*]pyrrole (13). Yellow solid. Yield: 0.12 g (6%). M.p. 330 °C (decomp.). ^1H NMR (500 MHz, CDCl_3) δ = 7.62 (d, J = 8.6 Hz, 4H), 7.36 (d, J = 8.6 Hz, 4H), 7.05 (d, J = 8.7 Hz, 4H), 6.63 (d, J = 8.8 Hz, 4H), 6.34 (s, 2H), 2.96 (s, 12H) ppm; ^{13}C { ^1H } NMR (126 MHz, CDCl_3) δ = 149.5, 144.0, 136.1, 133.1, 130.1, 129.4, 124.9, 120.7, 118.8, 112.2, 108.2, 95.6, 40.4 ppm. HRMS (EI): m/z calcd for $\text{C}_{36}\text{H}_{30}\text{N}_6$: 546.2532 [M^+]; found: 546.2536.

2,5-Bis(4-cyanophenyl)-1,4-bis(5,5,10,10,15-tetraethyltruxen-3-yl)-1,4-dihydropyrrolo[3,2-*b*]pyrrole (14). The compound was prepared starting from 4 mmol of parent aldehyde, 4 mmol of aniline, and 2 mmol of diacetyl. Yellow solid. Yield: 1.42 g (54%). M.p. > 400 °C. ^1H NMR (500 MHz, CDCl_3) δ = 8.50 (d, J = 8.4 Hz, 2H), 8.39 (d, J = 7.0 Hz, 2H), 8.25 (d, J = 6.6 Hz, 2H), 7.67 (dd, J = 8.3, 2.0 Hz, 2H), 7.55–7.45 (m, 12H), 7.45–7.35 (m, 8H), 7.00 (d, J = 2.0 Hz, 2H), 6.76 (s, 2H), 3.04 (dt, J = 13.8, 6.9 Hz, 8H), 2.94 (dt, J = 13.7, 6.9 Hz, 4H), 2.27–2.14 (m, 8H), 1.75 (dq, J = 14.0, 6.8 Hz, 4H), 0.29 (t, J = 7.2 Hz, 12H), 0.23 (t, J = 7.2 Hz, 12H), 0.19 (t, J = 7.2 Hz, 12H) ppm; ^{13}C { ^1H } NMR (126 MHz, CDCl_3) δ = 154.5, 152.8, 152.6, 144.3, 143.9, 143.7, 140.5, 140.3, 139.2, 139.1, 139.0, 137.9, 137.8, 137.4, 135.2, 133.2, 132.0, 128.3, 126.7, 126.3, 126.2, 125.5, 124.7, 124.4, 122.4, 122.3, 122.1, 120.0, 119.0, 109.3, 96.6, 56.8, 56.8, 56.8, 29.5, 29.4, 29.2, 8.7, 8.6, 8.5 ppm. HRMS (ESI): m/z calcd for $\text{C}_{98}\text{H}_{93}\text{N}_4$: 1325.7400 [$\text{M} + \text{H}^+$]; found: 1325.7390.

1,2,4,5-Tetrakis(4-methylphenyl)-1,4-dihydropyrrolo[3,2-*b*]pyrrole (15). White solid. Yield: 0.75g (40%). Spectral and optical properties concur with literature data.^{14a}

2,5-Bis(3-hydroxyphenyl)-1,4-bis(4-methylphenyl)-1,4-dihydropyrrolo[3,2-*b*]pyrrole (16). Off-white solid. Yield: 0.54 g (29%). M.p. 210 °C (decomp.). ^1H NMR (500 MHz, $\text{THF}-d_8$) δ = 8.09 (s, 2H), 7.17 (s, 8H), 6.99 (t, J = 8.0 Hz, 2H), 6.68 (d, J = 8.0 Hz, 2H), 6.61 (t, J = 1.5 Hz, 2H), 6.53 (dd, J = 8.0, 1.5 Hz, 2H), 6.30 (s, 2H), 2.34 (s, 6H) ppm. ^{13}C { ^1H } NMR (126 MHz, $\text{THF}-d_8$) δ = 157.4, 138.0,

135.5, 135.2, 134.6, 131.6, 129.3, 128.7, 124.6, 118.9, 114.6, 113.0, 94.6, 20.0 ppm. HRMS (EI): m/z calcd for $\text{C}_{32}\text{H}_{26}\text{N}_2\text{O}_2$: 470.1994 [M^+]; found: 470.2009.

2,5-Bis(2-benzyloxyphenyl)-1,4-bis(4-methylphenyl)-1,4-dihydropyrrolo[3,2-*b*]pyrrole (17). White solid. Yield: 0.96 g (37%). M.p. 197–198 °C. ^1H NMR (500 MHz, CDCl_3) δ = 7.31 (dd, J = 7.5, 1.5 Hz, 2H), 7.22–7.19 (m, 6H), 7.16–7.10 (m, 6H), 7.06–7.00 (m, 8H), 6.90 (t, J = 7.5 Hz, 2H), 6.74 (d, J = 8.0 Hz, 2H), 6.43 (s, 2H), 4.82 (s, 4H), 2.34 (s, 6H) ppm. ^{13}C { ^1H } NMR (126 MHz, CDCl_3) δ = 156.0, 138.6, 137.4, 134.0, 131.9, 131.6, 130.3, 129.3, 128.23, 128.19, 127.3, 126.6, 124.0, 123.5, 120.7, 113.0, 95.9, 70.2, 21.0 ppm. HRMS (EI): m/z calcd for $\text{C}_{46}\text{H}_{38}\text{N}_2\text{O}_2$: 650.2933 [M^+]; found: 650.2930.

2,5-Bis(4-methoxyphenyl)-1,4-bis(4-methylphenyl)-1,4-dihydropyrrolo[3,2-*b*]pyrrole (18). Beige solid. Yield: 0.60 g (30%). Spectral and optical properties concur with literature data.^{14a}

1,4-Bis(4-methylphenyl)-2,5-bis(1-tosylpyrrol-2-yl)-1,4-dihydropyrrolo[3,2-*b*]pyrrole (19). Pale yellow solid. Yield: 0.93 g (32%). M.p. 275–276 °C. ^1H NMR (500 MHz, CDCl_3) δ = 7.46 (d, J = 8.3 Hz, 4H), 7.43 (m, 2H), 7.13 (d, J = 8.2 Hz, 4H), 7.03 (d, J = 8.2 Hz, 4H), 6.88 (d, J = 8.3 Hz, 4H), 6.25 (t, J = 3.3 Hz, 2H), 6.16 (m, 2H), 5.82 (s, 2H), 2.33 (s, 6H), 2.31 (s, 6H) ppm; ^{13}C { ^1H } NMR (126 MHz, CDCl_3) δ = 144.9, 137.3, 136.1, 134.7, 129.4 (2x), 129.2, 127.8, 126.7, 123.6, 123.5, 123.3, 118.5, 111.3, 98.8, 21.6, 20.9 ppm. HRMS (EI): m/z calcd for $\text{C}_{42}\text{H}_{36}\text{N}_4\text{O}_4\text{S}_2$: 724.2178 [M^+]; found: 724.2170.

1,4-Bis(4-methylphenyl)-2,5-bis(thiophen-2-yl)-1,4-dihydropyrrolo[3,2-*b*]pyrrole (20). Yellow solid. Yield: 0.11g (6%). Spectral and optical properties concur with literature data.²⁷

1,4-Bis(4-(tert-butyl)phenyl)-2,5-bis(3-hydroxyphenyl)-1,4-dihydropyrrolo[3,2-*b*]pyrrole (21). Gray solid. Yield: 0.37g (17%). M.p. 280 °C. ^1H NMR (500 MHz, CDCl_3) δ = 7.36 (d, J = 8.5 Hz, 4H), 7.21 (d, J = 8.5 Hz, 4H), 7.09 (t, J = 7.9 Hz, 2H), 6.81 (d, J = 7.7 Hz, 2H), 6.69 (s, 2H), 6.65 (d, J = 8.2 Hz, 2H), 6.40 (s, 2H), 4.75 (s, 2H), 1.34 (s, 18H) ppm; ^{13}C { ^1H } NMR (126 MHz, CDCl_3) δ = 155.2, 148.5, 137.3, 135.3, 135.3, 131.7, 129.3, 125.9, 124.5, 120.8, 114.8, 113.1, 95.0, 34.5, 31.4 ppm. HRMS (EI): m/z calcd for $\text{C}_{38}\text{H}_{38}\text{N}_2\text{O}_2$: 554.2933 [M^+]; found: 554.2942.

1,4-Bis(4-tert-butylphenyl)-2,5-bis[4-(4-methoxybenzyloxy)phenyl]-1,4-dihydropyrrolo[3,2-*b*]pyrrole (22). Off-white solid. Yield: 1.12 g (35%). M.p. 268 °C (decomp.). ^1H NMR (500 MHz, CDCl_3) δ = 7.34 (d, J = 8.0 Hz, 8H), 7.19 (d, J = 8.0 Hz, 4H), 7.14 (d, J = 8.0 Hz, 4H), 6.90 (d, J = 8.0 Hz, 4H), 6.83 (d, J = 8.0 Hz, 4H), 6.32 (s, 2H), 4.95 (s, 4H), 3.81 (s, 6H), 1.33 (s, 18H) ppm; ^{13}C { ^1H } NMR (126 MHz, CDCl_3) δ = 159.4, 157.3, 148.2, 137.5, 135.1, 131.0, 129.4, 129.3, 129.0, 126.9, 125.8, 124.6, 114.5, 114.0, 94.0, 69.8, 55.3, 34.5, 31.4 ppm. HRMS (EI): m/z calcd for $\text{C}_{54}\text{H}_{54}\text{N}_2\text{O}_4$: 794.4084 [M^+]; found: 794.4044.

2,5-Bis(3,5-di-tert-butyl-4-hydroxyphenyl)-1,4-bis(4-methylphenyl)-1,4-dihydropyrrolo[3,2-*b*]pyrrole (23). Light-red solid. Yield: 0.90 g (32%). M.p. 195 °C (decomp.). ^1H NMR (500 MHz, CDCl_3) δ = 7.16 (s, 8H), 6.98 (s, 4H), 6.28 (s, 2H), 5.07 (s, 2H), 2.37 (s, 6H), 1.29 (s, 36H) ppm. ^{13}C { ^1H } NMR (126 MHz, CDCl_3) δ = 152.2, 137.9, 136.2, 135.2, 135.0, 130.6, 129.3, 125.5, 125.3, 124.8, 92.4, 34.2, 30.1, 20.9 ppm. HRMS (EI): m/z calcd for $\text{C}_{48}\text{H}_{58}\text{N}_2\text{O}_2$: 694.4498 [M^+]; found: 694.4438.

1,4-Bis(4-methylphenyl)-2,5-bis(pyrid-2-yl)-1,4-dihydropyrrolo[3,2-*b*]pyrrole (24). Yellow solid. Yield: 0.34 g (19%). M.p. 278–279 °C. ^1H NMR (500 MHz, CDCl_3) δ = 8.51 (d, J = 4.7 Hz, 2H), 7.38–7.45 (m, 2H), 7.22 (d, J = 8.2 Hz, 4H), 7.17 (d, J = 8.1 Hz, 4H), 7.02–6.95 (m, 4H), 6.77 (s, 2H), 2.38 (s, 5H), 2.35 (s, 1H) ppm; ^{13}C { ^1H } NMR (126 MHz, CDCl_3) δ = 151.9, 149.4, 137.8, 136.3, 135.7, 135.5, 133.4, 129.7, 129.0, 128.2, 125.2, 122.2, 120.4, 96.6, 21.0 ppm. HRMS (EI): m/z calcd for $\text{C}_{30}\text{H}_{24}\text{N}_4$: 440.2001 [M^+]; found: 440.1990.

1,4-Bis(4-octylphenyl)-2,5-bis(pyrid-2-yl)-1,4-dihydropyrrolo[3,2-*b*]pyrrole (25). Brown solid. Yield: 0.54 g (21%). M.p. 147 °C (decomp.). ^1H NMR (500 MHz, CDCl_3) δ = 8.51 (d, J = 4 Hz, 2H), 7.41 (t, J = 8.0 Hz, 2H), 7.23, 7.17 (AA'BB', J = 8.0 Hz, 8H), 7.01–6.98 (m, 2H), 6.96 (d, J = 8.0 Hz, 2H), 6.80 (s, 2H), 2.63 (t, J = 8.0 Hz, 4H), 1.70–1.60 (m, 4H), 1.40–1.20 (m, 20H), 0.89 (t, J = 6.5 Hz, 6H) ppm; ^{13}C { ^1H } NMR (126 MHz, CDCl_3) δ = 151.8, 149.3, 140.8, 137.8, 136.3, 135.5, 133.5, 129.0, 125.2, 122.2, 120.4, 96.8, 35.5, 31.9, 31.4,

29.5, 29.3, 22.7, 14.1 ppm. HRMS (EI): m/z calcd for $C_{44}H_{52}N_4$; 636.4192 [M^+]; found: 636.4195.

1,4-Bis(4-methylphenyl)-2,5-bis(pyridin-3-yl)-1,4-dihydropyrrolo[3,2-*b*]pyrrole (26). Yellow solid. Yield: 0.51 g (29%). Spectral and optical properties concur with literature data.^{14b}

1,4-Bis(4-methylphenyl)-2,5-bis(pyridin-4-yl)-1,4-dihydropyrrolo[3,2-*b*]pyrrole (27). Yellow solid. Yield: 0.33 g (19%). Spectral and optical properties concur with literature data.^{13a}

2,5-Bis(4-cyanophenyl)-1,4-bis(3-hydroxy-4-methylphenyl)-1,4-dihydropyrrolo[3,2-*b*]pyrrole (28). Yellow solid. Yield: 0.58 g (28%). M.p. 270 °C (decomp). ¹H NMR (500 MHz, THF-*d*₈) δ = 8.67 (br s, 2H), 7.54 (d, *J* = 8.3 Hz, 4H), 7.38 (d, *J* = 8.3 Hz, 4H), 7.12 (d, *J* = 7.9 Hz, 2H), 6.68 (dd, *J* = 7.8, 1.8 Hz, 2H), 6.62 (d, *J* = 1.7 Hz, 2H), 6.55 (s, 2H), 2.21 (s, 6H) ppm; ¹³C {¹H} NMR (126 MHz, THF-*d*₈) δ = 157.3, 139.1, 138.8, 135.8, 134.8, 132.7, 132.1, 128.5, 123.9, 119.3, 116.8, 112.5, 110.0, 96.9, 15.9 ppm. HRMS (EI): m/z calcd for $C_{34}H_{24}N_4O_2$; 520.1899 [M^+]; found: 520.1919.

2,5-Bis(4-methylphenyl)-1,4-bis(4-nitrophenyl)-1,4-dihydropyrrolo[3,2-*b*]pyrrole (29). Red solid. Yield: 0.26 g (25%). Spectral and optical properties concur with literature data.^{14a}

2,5-Bis(2-methoxyphenyl)-1,4-bis(4-methylphenyl)-1,4-dihydropyrrolo[3,2-*b*]pyrrole (30). Beige solid. Yield: 1.01 g (51%). Spectral and optical properties concur with literature data.^{14b}

1,4-Bis(2-bromophenyl)-2,5-bis(4-trifluoromethylphenyl)-1,4-dihydropyrrolo[3,2-*b*]pyrrole (31). Pale yellow solid. Yield: 0.86 g (31%). M.p. 314–315 °C. ¹H NMR (500 MHz, CDCl₃), mixture of atropoisomers, δ = 7.78–7.73 (m, 2H), 7.41 (d, *J* = 8.3 Hz, 4H), 7.37–7.14 (m, 10H), 6.37, 6.35 (2x s, 2H) ppm; ¹³C {¹H} NMR (126 MHz, CDCl₃) δ = 139.2, 136.7 (m), 134.0, 133.9, 133.1, 132.9, 130.4, 130.3, 129.3, 129.2, 128.4, 128.3, 127.9, 127.6, 127.2, 127.1, 125.2 (q, *J* = 4 Hz), 123.2, 121.9, 121.3, 96.0, 95.6 ppm. HRMS (EI): m/z calcd for $C_{32}H_{18}N_4F_6Br_2$; 701.9741 [M^+]; found: 701.9727.

1,4-Bis(2-cyanophenyl)-2,5-bis(4-trifluoromethylphenyl)-1,4-dihydropyrrolo[3,2-*b*]pyrrole (32). White solid. Yield: 0.23 g (10%). M.p. 309 °C (decomp). ¹H NMR (500 MHz, CDCl₃), mixture of atropoisomers, δ = 7.82–7.76 (m, 2H), 7.70–7.58 (m, 2H), 7.50–7.38 (m, 8H), 7.30–7.22 (m, 4H), 7.54 (s, 0.5H), 7.49 (s, 1.5H) ppm. ¹³C {¹H} NMR (126 MHz, CDCl₃) δ = 142.3, 142.1, 136.7, 136.6, 136.0, 134.1 (q, *J* = 28.6 Hz), 133.0, 132.9, 128.8, 128.5, 128.4, 128.3, 127.72, 127.68, 127.5, 127.3, 125.4 (q, 3.7 Hz), 124.2 (q, *J* = 272 Hz), 116.3, 116.0, 112.0, 110.6, 110.5, 97.5, 97.2 ppm. HRMS (EI): m/z calcd for $C_{34}H_{18}F_6N_4$; 596.1436 [M^+]; found: 596.1450.

1,4-Bis(2-chlorophenyl)-2,5-bis(4-pentafluorosulfanylphenyl)-1,4-dihydropyrrolo[3,2-*b*]pyrrole (33). White solid. Yield: 0.87 g (26%). M.p. 315–317 °C. ¹H NMR (500 MHz, THF-*d*₆), mixture of atropoisomers, δ = 7.66 (dd, *J* = 8.0, 1.3 Hz, 1H), 7.65–7.60 (m, 5H), 7.48–7.39 (m, 4H), 7.36 (td, *J* = 7.7, 1.4 Hz, 1H), 7.30 (d, *J* = 7.9 Hz, 4H), 7.26 (dd, *J* = 7.8, 1.5 Hz, 1H), 6.51 (s, 1H), 6.48 (s, 1H) ppm. ¹³C {¹H} NMR (126 MHz, THF-*d*₆) δ = 152.2 (m), 138.5, 138.5, 137.9, 137.8, 137.3, 137.1, 137.0, 134.7, 134.5, 132.7, 132.6, 131.7, 131.6, 131.2, 131.1, 130.3, 130.2, 129.0, 128.9, 127.5, 127.4, 126.8 (m), 97.3, 96.7 ppm. HRMS (EI): m/z calcd for $C_{30}H_{18}N_2S_2Cl_2F_{10}$; 730.0129 [M^+]; found: 730.0143.

2,5-Bis(anthracen-9-yl)-1,4-bis(4-octylphenyl)-1,4-dihydropyrrolo[3,2-*b*]pyrrole (34). Yellow solid. Yield: 1.02 g (31%). Spectral and optical properties concur with literature data.^{13b}

2,5-Bis(6,7-dimethoxy-2H-chromen-2-on-4-yl)-1,4-bis(4-octylphenyl)-1,4-dihydropyrrolo[3,2-*b*]pyrrole (35). Yellow solid. Yield: 0.70 g (39%). M.p. 181–182 °C. ¹H NMR (500 MHz, CDCl₃) δ 7.22 (d, *J* = 8.4 Hz, 4H), 7.14 (d, *J* = 8.4 Hz, 4H), 7.05 (s, 2H), 6.83 (s, 2H), 6.65 (s, 2H), 6.17 (s, 2H), 3.92 (s, 6H), 3.71 (s, 6H), 2.62–2.53 (m, 4H), 1.61–1.53 (m, 4H), 1.31–1.22 (m, 20H), 0.87 (t, *J* = 7.0 Hz, 6H) ppm. ¹³C {¹H} NMR (126 MHz, CDCl₃) δ 161.2, 152.7, 150.0, 146.7, 145.9, 141.7, 136.4, 132.8, 130.9, 129.6, 123.4, 112.6, 110.8, 108.0, 100.1, 98.5, 56.5, 56.3, 35.3, 31.9, 29.4, 29.2 (2 signals), 22.6, 14.1 ppm. HRMS (EI): m/z calcd for $C_{56}H_{62}N_2O_8$; 890.4506 [M^+]; found: 890.4487.

2,5-Bis(4-nitrophenyl)-1,4-bis(4-octylphenyl)-1,4-dihydropyrrolo[3,2-*b*]pyrrole (36). Red solid. Yield: 1.19 g (41%). Spectral and optical properties concur with literature data.^{13c}

1,4-Bis(3,5-di-*tert*-butylphenyl)-2,5-bis(fluoranthene-3-yl)-1,4-dihydropyrrolo[3,2-*b*]pyrrole (37). Compound was prepared starting from 0.25 mmol of parent aldehyde, 0.25 mmol of aniline, and 0.125 mmol of butan-2,3-dione. Orange solid. Yield: 45 mg (41%). Spectral and optical properties concur with literature data.^{13b}

2,5-Bis(8-hydroxy-quinolin-4-yl)-1,4-bis(4-octylphenyl)-1,4-dihydropyrrolo[3,2-*b*]pyrrole (38). Yellow solid. Yield: 0.32 g (10%). M.p. 251–252 °C. ¹H NMR (500 MHz, CDCl₃) δ = 8.71 (dd, *J* = 4.1, 1.5 Hz, 2H), 8.41 (dd, *J* = 8.6, 0.9 Hz, 2H), 7.38 (d, *J* = 7.9 Hz, 2H), 7.30 (dd, *J* = 8.6, 4.1 Hz, 2H), 7.11 (d, *J* = 7.9 Hz, 2H), 7.08 (d, *J* = 8.4 Hz, 4H), 6.97 (d, *J* = 8.5 Hz, 4H), 6.46 (s, 2H), 2.48 (t, *J* = 7.7 Hz, 4H), 1.56–1.46 (m, 4H), 1.32–1.18 (m, 22H), 0.87 (t, 6H, *J* = 7.0 Hz) ppm. ¹³C {¹H} NMR (126 MHz, CDCl₃) δ = 151.7, 147.6, 140.0, 138.2, 137.4, 135.3, 132.0, 130.4, 130.1, 128.8, 127.7, 123.9, 122.4, 121.7, 109.4, 96.6, 35.3, 31.8, 31.2, 29.4, 29.2, 22.6, 14.1 ppm. HRMS (EI): m/z calcd for $C_{52}H_{56}N_4O_2$; 768.4403 [M^+]; found: 68.4371.

2,5-Bis(3,4-dicyano-5-methyl-1H-pyrrol-2-yl)-1,4-bis(4-octylphenyl)-1,4-dihydropyrrolo[3,2-*b*]pyrrole (39). Yellow solid. Yield: 0.85 g (29%). M.p. 325 °C (decomp). ¹H NMR (500 MHz, THF-*d*₆) δ = 11.07 (s, 2H), 7.15, 7.07 (AA'BB', *J* = 8.5 Hz, 8H), 6.51 (s, 2H), 2.55 (t, *J* = 7.0 Hz, 4H), 2.18 (s, 6H), 1.60–1.50 (m, 4H), 1.30–1.10 (m, 20H), 0.79 (t, *J* = 7 Hz, 6H) ppm. ¹³C {¹H} NMR (126 MHz, THF-*d*₆) δ = 141.1, 138.9, 136.5, 131.8, 131.5, 129.2, 123.9, 123.7, 112.75, 112.71, 97.0, 94.5, 93.9, 35.2, 31.8, 31.3, 29.4, 29.3, 29.2, 22.5, 13.4, 10.7 ppm. HRMS (EI): m/z calcd for $C_{48}H_{52}N_8$; 740.4315 [M^+]; found: 740.4292.

1,4-Bis(2-bromophenyl)-2,5-bis(3,5-bis(trifluoromethyl)phenyl)-1,4-dihydropyrrolo[3,2-*b*]pyrrole (40). Pale yellow solid. Yield: 0.22 g (7%). M.p. 220–221 °C. ¹H NMR (500 MHz, CDCl₃), mixture of atropoisomers, δ = 7.78–7.73 (m, 2H), 7.57 (s, 2H), 7.56 (s, 4H), 7.42–7.26 (m, 6H), 6.45 (s, 1H), 6.44 (s, 1H) ppm. ¹³C {¹H} NMR (126 MHz, CDCl₃) δ = 138.4, 138.4, 135.5, 135.4, 135.0, 134.9, 134.2, 134.1, 133.2, 133.0, 131.6 (2x q, *J* = 34 Hz), 131.4, 130.2, 130.1, 130.0, 129.9, 128.7, 128.6, 126.7 (m), 124.2, 122.4, 122.3, 122.1, 119.3 (m), 95.7, 95.3 ppm. HRMS (EI): m/z calcd for $C_{34}H_{16}N_2F_{12}Br_2$; 839.9468 [M^+]; found: 839.9501.

1,4-Bis(2-chlorophenyl)-2,5-bis(3,5-bis(trifluoromethyl)phenyl)-1,4-dihydropyrrolo[3,2-*b*]pyrrole (41). Pale yellow solid. Yield: 0.36 g (12%). M.p. 199–200 °C. ¹H NMR (500 MHz, CDCl₃), mixture of atropoisomers, δ = 7.60–7.54 (m, 8H), 7.42–7.31 (m, 5H), 7.27–7.25 (m, 1H), 6.45 (s, 1H), 6.44 (s, 1H) ppm. ¹³C {¹H} NMR (126 MHz, CDCl₃) δ = 136.7, 136.7, 135.5, 135.4, 135.0, 134.9, 133.2, 133.0, 132.1, 132.1, 131.7 (2x q, *J* = 34 Hz), 131.0, 130.9, 130.0, 129.9, 129.7, 129.6, 128.0, 128.0, 126.6 (m), 123.1 (q, *J* = 272 Hz), 119.4 (m), 95.8, 95.4 ppm. HRMS (EI): m/z calcd for $C_{34}H_{16}N_2F_{12}Cl_2$; 750.0499 [M^+]; found: 750.0490.

1,4-Bis(4-methylphenyl)-2,5-bis(3,5-bis(trifluoromethyl)phenyl)-1,4-dihydropyrrolo[3,2-*b*]pyrrole (42). Pale orange solid. Yield: 1.15 g (57%). M.p. 279–280 °C. ¹H NMR (500 MHz, CDCl₃) δ = 7.59 (d, *J* = 8.3 Hz, 6H), 7.24 (d, *J* = 8.2 Hz, 4H), 7.16 (d, *J* = 8.2 Hz, 4H), 6.50 (s, 2H), 2.41 (s, 6H) ppm; ¹³C {¹H} NMR (126 MHz, CDCl₃) δ = 137.1, 136.3, 135.2, 133.9, 133.1, 131.4 (q, *J* = 33.3 Hz), 130.3, 127.3 (m), 125.5, 124.3, 119.2 (m), 95.4, 21.0 ppm. HRMS (EI): m/z calcd for $C_{36}H_{22}F_{12}N_2$; 710.1591 [M^+]; found: 710.1594.

1,4-Bis(4-hexylphenyl)-2,5-bis(5-(4-nitrophenyl)thiophen-2-yl)-1,4-dihydropyrrolo[3,2-*b*]pyrrole (43). Brownish solid. Yield: 0.24 g (28%). M.p. 215–216 °C. ¹H NMR (500 MHz, CDCl₃) δ = 8.18 (d, *J* = 8.9 Hz, 4H), 7.59 (d, *J* = 8.9 Hz, 4H), 7.34 (d, *J* = 8.3 Hz, 4H), 7.29 (d, *J* = 8.3 Hz, 4H), 7.23 (d, *J* = 3.9 Hz, 2H), 6.60 (d, *J* = 3.9 Hz, 2H), 6.41 (s, 2H), 2.70 (t, *J* = 7.8 Hz, 4H), 1.74–1.65 (m, 4H), 1.42–1.29 (m, 12H), 0.91 (t, *J* = 7.0 Hz, 6H) ppm; ¹³C {¹H} NMR (126 MHz, CDCl₃) δ = 142.4, 140.4, 138.8, 138.4, 138.1, 136.6, 133.0, 130.2, 129.4, 126.4, 126.1, 125.5, 125.2, 124.4, 94.2, 35.6, 31.7, 31.3, 28.9, 22.6, 14.1 ppm; HRMS (EI): m/z calcd for $C_{50}H_{48}N_4S_2O_4$; 832.3117 [M^+]; found: 832.3085.

1,4-Bis(2H-chromen-2-on-6-yl)-2,5-bis(3,5-bis(trifluoromethyl)phenyl)-1,4-dihydropyrrolo[3,2-*b*]pyrrole (44). Off-white solid. Yield: 0.28 g (34%). M.p. 359–360 °C. ¹H NMR (500 MHz, THF-*d*₈) δ = 7.85 (d, *J* = 9.5 Hz, 2H), 7.82–7.77 (m, 6H), 7.67 (d, *J* = 2.2 Hz, 2H), 7.50 (dd, *J* = 8.8, 2.2 Hz, 2H), 7.43 (d, *J* = 8.8 Hz, 2H), 6.85 (s, 2H), 6.46 (d, *J* = 9.5 Hz, 2H) ppm; ¹³C {¹H} NMR (126 MHz, THF-*d*₈) δ =

158.6, 152.8, 142.1, 135.2, 135.1, 134.1, 133.6, 131.3 (q, $J = 131.5$ Hz), 128.9, 127.3, 124.4, 122.2, 119.9, 119.3, 117.8, 117.7, 96.5 ppm; HRMS (EI): m/z calcd for $C_{40}H_{18}N_2F_{12}O_4$: 818.1075 [M^+]; found: 818.1108.

1,4-Bis(4-*n*-decylphenyl)-2,5-bis(4-(1,3-dioxoisindol-2-yl)phenyl)-1,4-dihydropyrrolo[3,2-*b*]pyrrole (45). Yellow solid. Yield: 1.45 g (37%). M.p. 218 °C. 1H NMR (500 MHz, $CDCl_3$) $\delta = 7.93$ (m, 4H), 7.77 (m, 4H), 7.35 (d, $J = 8.5$ Hz, 4H), 7.31 (d, $J = 8.6$ Hz, 4H), 7.24 (d, $J = 8.5$ Hz, 4H), 7.20 (d, $J = 8.3$ Hz, 4H), 6.44 (s, 2H), 2.68–2.60 (m, 4H), 1.68–1.62 (m, 4H), 1.40–1.20 (m, 28H), 0.87 (t, $J = 6.8$ Hz, 6H) ppm; ^{13}C { 1H } NMR (126 MHz, $CDCl_3$) $\delta = 167.3, 140.7, 137.4, 135.2, 134.4, 133.5, 132.2, 131.8, 129.4, 129.2, 128.3, 126.0, 125.2, 123.7, 95.1, 35.5, 31.9, 31.3, 29.6, 29.6, 29.5, 29.4, 29.3, 22.7, 14.1$ ppm. HRMS (EI): m/z calcd for $C_{66}H_{68}N_4O_4$: 980.5241 [M^+]; found: 980.5265.

1,4-Bis(3,5-di-(*tert*-butyl)phenyl)-2,5-bis(4-(methylsulfinyl)phenyl)-1,4-dihydropyrrolo[3,2-*b*]pyrrole (46). Pale green solid. Yield: 1.38 g (45%). M.p. 319–320 °C. 1H NMR (500 MHz, $CDCl_3$) $\delta = 7.50$ (d, $J = 8.3$ Hz, 4H), 7.34 (d, $J = 8.3$ Hz, 4H), 7.31–7.27 (m, 2H), 7.08 (d, $J = 1.6$ Hz, 4H), 6.48 (s, 2H), 2.67 (s, 6H), 1.23 (s, 36H) ppm; ^{13}C { 1H } NMR (126 MHz, $CDCl_3$) $\delta = 151.9, 143.0, 138.6, 136.8, 135.0, 132.0, 129.0, 123.3, 119.8, 119.6, 95.0, 44.1, 34.9, 31.3$ ppm. HRMS (EI): m/z calcd for $C_{48}H_{58}N_2S_2O_2$: 758.3940 [M^+]; found: 758.3926.

1,4-Bis(2-bromophenyl)-2,5-bis(3,5-di(trifluoromethyl)phenyl)-1,4-dihydropyrrolo[3,2-*b*]pyrrole (49). Pale yellow solid. Yield: 0.25 g (7%). M.p. 259–260 °C. 1H NMR (500 MHz, $CDCl_3$, mixture of atropoisomers) $\delta = 7.75$ –7.71 (m, 2H), 7.55 (bs, 2H), 7.51 (bs, 4H), 7.44–7.33 (m, 3H), 7.20 (d, $J = 8.2$ Hz, 1H), 6.46 (2 \times s, 2H), 1.36 (2 \times s, 18H) ppm; ^{13}C { 1H } NMR (126 MHz, $CDCl_3$) $\delta = 154.1, 154.0, 135.5, 135.5, 135.3, 135.1, 135.0, 133.1, 132.9, 131.4$ (2 \times q, $J = 34$ Hz), 131.04, 130.98, 129.6, 129.5, 126.6 (m), 125.8, 125.7, 123.2 (q, $J = 273$ Hz), 122.1, 122.0, 119.1 (m), 95.2, 94.9, 34.93, 34.92, 31.1, 29.7 ppm. HRMS (EI): m/z calcd for $C_{42}H_{32}N_2F_{12}Br_2$: 950.0741 [M^+]; found: 950.0743.

Synthesis of π -Expanded Dihydropyrrolo[3,2-*b*]pyrrole 50. Parent TAPP (49, 142.5 mg, 0.15 mmol), CS_2CO_3 (117.3 mg, 0.36 mmol), PPh_3 (9 mg, 0.035 mmol), and 9 mL of dry toluene were placed in the Schlenk flask. Subsequently, the solution of $Pd(OAc)_2$ in N,N -dimethylacetamide (DMA, 3.4 mL, 1 mg/mL, 10 mol %) was added and the reaction was stirred at 120 °C (oil bath) for 2 h. After cooling, the resulting precipitate was washed three times alternately with $CHCl_3$ and water to afford 107 mg (91%) of the expected product as an orange solid (poor solubility in common organic solvents). Orange solid. Yield: 109 mg (92%). M.p. 390–391 °C. 1H NMR (600 MHz, THF- d_8) $\delta = 8.89$ (s, 2H), 8.48 (s, 2H), 8.40 (d, $J = 8.6$ Hz, 1H), 8.11 (s, 2H), 8.10 (s, 2H), 7.85 (dd, $J = 8.5$ Hz, 2.0 Hz, 2H), 1.46 (s, 18H) ppm; ^{13}C { 1H } NMR (151 MHz, THF- d_8) $\delta = 146.5, 134.4, 132.5, 131.5, 130.1, 129.9, 129.6, 129.3, 129.0, 128.1, 127.8$ (m), 125.8, 124.5 (m), 123.4 (m), 118.9, 116.0, 91.0, 35.6, 31.6, 30.6 ppm; ^{19}F NMR (470 MHz, THF- d_8) $\delta = -55.64, -63.63$ ppm. HRMS (EI): m/z calcd for $C_{42}H_{30}N_2F_{12}$: 970.2217 [M^+]; found: 970.2222.

Synthesis of Annulated Dihydropyrrolo[3,2-*b*]pyrrole 51. In a Schlenk flask containing a magnetic stirring bar, 7a (61.4 mg, 0.12 mmol) and $InCl_3$ (5.3 mg, 0.024 mmol) were placed. The vessel was evacuated and backfilled with argon (three times), and anhydrous toluene was added (60 mL). The vessel was tightly closed and again carefully evacuated (until the mixture started to boil) and backfilled with argon. The resulting mixture was heated at 110 °C (oil bath) for 16 h. After reaction completion, the volatiles were filtered off and the crude product was purified by means of flash column chromatography (DCM/hexanes = 1:1) and recrystallized (DCM/hexanes) to afford 21.6 mg (35%) of pure 51. Yellow solid. Yield: 21.6 mg (35%) M.p. 210 °C (decomp.). 1H NMR (600 MHz, $CDCl_3$) $\delta = 7.58$ (d, $J = 7.9$ Hz, 3H), 7.49 (d, $J = 8.1$ Hz, 2H), 7.46 (d, $J = 8.0$ Hz, 2H), 7.31–7.27 (m, 2H), 7.16 (d, $J = 8.1$ Hz, 2H), 7.03–6.97 (m, 1H), 6.93 (d, $J = 7.3$ Hz, 1H), 6.88 (t, $J = 7.4$ Hz, 1H), 6.81 (t, $J = 7.5$ Hz, 1H), 6.42 (d, $J = 8.1$ Hz, 1H), 6.23 (s, 1H), 6.15 (d, $J = 11.3$ Hz, 1H), 6.05 (d, $J = 11.3$ Hz, 1H), 3.13 (s, 1H) ppm; ^{13}C { 1H } NMR (151 MHz, $CDCl_3$) $\delta = 141.5, 141.4, 139.5, 138.6, 136.0, 135.7, 134.4, 134.1, 133.4, 132.8, 132.3, 132.0, 130.7, 130.3, 129.9, 128.9, 128.7, 127.7, 127.5, 127.3, 125.0, 123.6,$

123.3, 119.8, 119.0, 118.9, 112.8, 109.7, 109.5, 103.2, 83.4, 79.8 ppm. HRMS (EI): m/z calcd for $C_{36}H_{20}N_4$: 508.1688 [M^+]; found: 508.1685.

Synthesis of 2,5-Bis(2-methoxyphenyl)-1,4-bis(4-methylphenyl)-3-(tricyanovinyl)-1,4-dihydropyrrolo[3,2-*b*]pyrrole (52) and Tetra-cyanoethylene-Derived Adduct (53). Pyrrolopyrrole 30 (250 mg, 0.5 mmol) was dissolved in hot toluene (20 mL), and TCNE (256 mg, 2 mmol) was added, followed by pyridine (0.5 mL). The resulting brown mixture was heated at 110 °C (oil bath) for 3 h. Then, the solvent was removed and the residue was loaded onto the column and chromatographed (silica, DCM/hexanes, 3:2). The first two colored (yellow and black) bands were collected, evaporated separately, and triturated with hot MeOH to afford 52 (73 mg, 24%) and 53 (155 mg, 54%). Compound 52. Black solid. Yield: 73 mg (24%). M.p. 270–271 °C. 1H NMR (500 MHz, $CDCl_3$) $\delta = 7.21$ (d, $J = 8.5$ Hz, 2H), 7.18 (d, $J = 8.5$ Hz, 2H), 7.13 (d, $J = 8.5$ Hz, 2H), 7.08–7.02 (m, 6H), 6.88 (d, $J = 8.5$ Hz, 2H), 6.76 (d, $J = 8.5$ Hz, 2H), 6.24 (s, 1H), 3.82 (s, 3H), 3.78 (s, 3H), 2.43 (s, 3H), 2.38 (s, 3H) ppm; ^{13}C { 1H } NMR (126 MHz, $CDCl_3$) $\delta = 160.6, 158.9, 140.3, 138.8, 138.0, 137.9, 135.3, 135.0, 133.7, 132.4, 132.0, 130.4, 130.0, 129.3, 127.7, 125.6, 125.1, 124.9, 121.5, 114.5, 113.6, 112.9, 111.9, 111.6, 101.8, 93.5, 89.3, 55.3, 55.2, 21.2, 21.1$ ppm. HRMS (EI): m/z calcd for $C_{39}H_{29}N_5O_2$: 599.2321 [M^+]; found: 599.2323.

Compound 53. Yellow solid. Yield: 155 mg (54%). M.p. 230 °C (decomp.). 1H NMR (500 MHz, $CDCl_3$) $\delta = 7.34$ (br d, $J = 2$ Hz, 5H), 7.29 (br s, 3H + 1H covered with $CDCl_3$), 7.06 (d, $J = 8.5$ Hz, 2H), 6.85 (dd, $J = 9.0, 2.5$ Hz, 1H), 6.81 (d, $J = 9.0$ Hz, 1H), 6.76 (d, $J = 8.5$ Hz, 2H), 6.22 (s, 1H), 3.87 (s, 3H), 3.79 (s, 3H), 2.48 (s, 3H), 2.45 (s, 3H) ppm; ^{13}C { 1H } NMR (126 MHz, $CDCl_3$) $\delta = 158.9, 158.4, 140.5, 138.6, 138.15, 136.5, 135.9, 134.6, 130.66, 130.64, 129.9, 126.5, 125.8, 125.5, 125.3, 124.9, 120.3, 119.8, 117.5, 113.8, 113.6, 110.8, 109.8, 92.1, 55.7, 55.2, 21.24, 21.21$ ppm. HRMS (EI): m/z calcd for $C_{40}H_{28}N_6O_2$: 624.2274 [M^+]; found: 624.2259.

Synthesis of 1,4-Bis(4-octylphenyl)-2,5-bis(pyrid-2-yl)-1,4-dihydropyrrolo[3,2-*b*]pyrrole BMes₂-Chelate (54). Pyrrolopyrrole 25 (318 mg, 0.5 mmol) was dissolved in dry THF (45 mL) in a dried Schlenk flask. The mixture was cooled to –78 °C, and *n*-BuLi (2.5 M solution in hexane, 0.4 mL, 1 mmol) was slowly added over a period of 5 min. After stirring at –78 °C for 1 h, $BMes_2F$ (295 mg, 1.1 mmol) in THF (5 mL) was slowly added and the reaction mixture was allowed to warm to room temperature and stirred for 6 h. The solvents were removed under reduced pressure, and the resulting solid was dissolved in CH_2Cl_2 and quenched with 10 mL of H_2O . The organic layer was separated and dried over $MgSO_4$ and filtered. After CH_2Cl_2 was removed under reduced pressure, the residue was loaded onto the column and chromatographed (silica, DCM/hexanes, 3:2). A green fluorescent band was collected, evaporated, and crystallized from $CHCl_3$ /MeOH to give yellow crystals of 54. Yellow solid. Yield: 295 mg (67%). M.p. 89–90 °C. 1H NMR (500 MHz, $CDCl_3$) $\delta = 8.43$ (t, $J = 6.5$ Hz, 2H), 7.41–7.37 (m, 3H), 7.30 (d, $J = 8.0$ Hz, 2H), 7.16 (t, $J = 7.5$ Hz, 1H), 6.91 (d, $J = 8.0$ Hz, 2H), 6.88 (t, $J = 8.5$ Hz, 2H), 6.82 (d, $J = 8.0$ Hz, 2H), 6.66 (t, $J = 6.5$ Hz, 2H), 6.53 (s, 4H), 6.22 (d, $J = 8.0$ Hz, 1H), 2.69 (t, $J = 8.0$ Hz, 2H), 2.59 (t, $J = 8.0$ Hz, 2H), 2.18 (s, 6H), 1.68 (s, 12H), 1.66–1.60 (m, 4H), 1.40–1.20 (m, 20H), 0.89 (dt, $J = 7.0, 1.5$ Hz, 6H) ppm; ^{13}C { 1H } NMR (126 MHz, $CDCl_3$) $\delta = 151.2, 149.2, 145.3, 142.4, 141.5, 141.0, 139.9, 138.7, 137.4, 136.9, 135.0, 134.6, 133.3, 129.6, 129.3, 129.2, 129.0, 125.5, 121.9, 120.4, 116.3, 115.7, 35.61, 35.58, 31.9, 31.5, 31.4, 29.49, 29.47, 29.31, 22.7, 20.7, 14.1$ ppm. HRMS (ESI): m/z calcd for $C_{62}H_{74}BN_4$: 885.6015 [$M+H^+$]; found: 885.6007.

General Procedure for the Large-Scale Preparation of Tetraarylpyrrolo[3,2-*b*]pyrroles. A three-necked, 250 mL round-bottomed flask was equipped with a 5 cm Teflon-coated football-shaped magnetic stir bar. The flask was charged with 70 mL of acetic acid and 70 mL of toluene, followed by the addition of aldehyde (80.0 mmol, 2.0 equiv) and aniline (80 mmol, 2 equiv). The flask was immersed in a silicone oil bath preheated to 50 °C. The clear solution was stirred for 30 min under an air atmosphere. Then, quickly weighed iron(III) perchlorate hydrate (0.85 g, 2.4 mmol, 6 mol %) was added, causing immediate reddening of the solution. Shortly after the addition

of perchlorate, butane-2,3-dione (3.45 g, 3.5 mL, 40 mmol, 1 equiv) was added, dropwise, over 3 min. The mixture was heated at 50 °C (temperature of the oil bath was 65 °C, and the thermometer immersed in the reaction mixture showed 50 °C). After few minutes, plenty of precipitates were formed and the resulting suspension was vigorously stirred for 16 h at 50 °C with all three necks uncapped throughout the whole reaction time to provide access of the oxygen from the air. Then, the oil bath was removed to allow the reaction mixture to cool to room temperature over 15 min. The resulting dark mixture was filtered, the precipitate was rinsed with methanol (2 × 250 mL) and a small amount of diethyl ether, and dried under vacuum (oil pump, argon/vacuum line, 0.80 mmHg) at 95 °C for 3 h to give the desired pyrrolopyrrole. In the case of pyrrolopyrroles synthesized from pyridinecarbaldehydes, the products do not precipitate; therefore, the workup was as follows: the reaction mixture was transferred to 500 mL RBF, and the solvents were removed under reduced pressure. Fifty milliliters of toluene was added to the resulting dark oil, and the mixture was evaporated again to remove traces of acetic acid, which facilitates crystallization. Fifty milliliters of acetonitrile was added to the obtained dark oil, and the whole mixture was boiled for 1 min, which caused the formation of large quantities of precipitates. The flask was allowed to stand at r.t. for 15 min and then transferred to the fridge for 3 h. Subsequent filtration and drying under high vacuum afforded the desired pyridine-substituted pyrrolopyrrole.

Photophysical Measurements. All photophysical studies have been performed with freshly prepared air-equilibrated solutions at room temperature (298 K). A Perkin-Elmer Lambda 25 UV/vis spectrophotometer and a Hitachi F7000 fluorescence spectrometer were used to acquire the absorption and emission spectra. Spectroscopic-grade solvents were used without further purification. Quantum yields were estimated by measuring the fluorescence and absorbance of samples and a dye reference in DCM, MeCN, and EtOH and for selected examples in water.

ASSOCIATED CONTENT

Supporting Information

The Supporting Information is available free of charge at <https://pubs.acs.org/doi/10.1021/acs.joc.0c01665>.

Optical properties; copies of ¹H and ¹³C{¹H} NMR data; determination of the structure of compound **51**; X-ray crystallographic information; and photophysical data (PDF)

X-ray crystal data for **50** (CIF)

X-ray crystal data for **53** (CIF)

AUTHOR INFORMATION

Corresponding Author

Daniel T. Gryko – Institute of Organic Chemistry, Polish Academy of Sciences, 01-224 Warsaw, Poland; orcid.org/0000-0002-2146-1282; Email: dtgryko@icho.edu.pl

Authors

Mariusz Tasior – Institute of Organic Chemistry, Polish Academy of Sciences, 01-224 Warsaw, Poland

Olena Vakuliuk – Institute of Organic Chemistry, Polish Academy of Sciences, 01-224 Warsaw, Poland

Daiki Koga – Institute of Organic Chemistry, Polish Academy of Sciences, 01-224 Warsaw, Poland

Beata Koszarna – Institute of Organic Chemistry, Polish Academy of Sciences, 01-224 Warsaw, Poland

Krzysztof Górski – Institute of Organic Chemistry, Polish Academy of Sciences, 01-224 Warsaw, Poland

Marek Grzybowski – Institute of Organic Chemistry, Polish Academy of Sciences, 01-224 Warsaw, Poland

Łukasz Kielesiński – Institute of Organic Chemistry, Polish Academy of Sciences, 01-224 Warsaw, Poland

Maciej Krzeszewski – Institute of Organic Chemistry, Polish Academy of Sciences, 01-224 Warsaw, Poland

Complete contact information is available at: <https://pubs.acs.org/10.1021/acs.joc.0c01665>

Author Contributions

M.T., O.V., and D.K. contributed equally. The manuscript was written through the contributions of all authors.

Notes

The authors declare no competing financial interest.

ACKNOWLEDGMENTS

The authors would like to thank the Foundation for Polish Science (TEAM POIR.04.04.00-00-3CF4/16-00), COST (CHAOS CA 15106), and Global Research Laboratory Program (2014K1A1A2064569) through the National Research Foundation (NRF) funded by the Ministry of Science, ICT & Future Planning (Korea). The authors thank Dr. David C. Young for amending the manuscript.

REFERENCES

- (1) (a) Narita, A.; Wang, X.-Y.; Feng, X.; Müllen, K. New Advance in Nanographene Chemistry. *Chem. Soc. Rev.* **2015**, *44*, 6616–6643. (b) Bunz, U. H. F. The Larger Linear N-Heteroacenes. *Acc. Chem. Res.* **2015**, *48*, 1676–1686. (c) Ito, S.; Tokimaru, Y.; Nozaki, K. Benzene-Fused Azacorannulene Bearing an Internal Nitrogen Atom. *Angew. Chem., Int. Ed.* **2015**, *54*, 7256–7260. (d) Stepien, M.; Gońka, E.; Żyła, M.; Sprutta, N. Heterocyclic Nanographenes and Other Polycyclic Heteroaromatic Compounds: Synthetic Routes, Properties and Applications. *Chem. Rev.* **2017**, *117*, 3479–3716. (e) Chen, F.; Hong, Y. S.; Shimizu, S.; Kim, D.; Tanaka, T.; Osuka, A. Synthesis of a Tetrabenzotetraaza[8]circulene by a “Fold-In” Oxidative Fusion Reaction. *Angew. Chem., Int. Ed.* **2015**, *54*, 10639–10642.
- (2) (a) Oki, K.; Takase, M.; Mori, S.; Uno, H. Synthesis and Isolation of Antiaromatic Expanded Azacoronene via Intramolecular Vilsmeier-Type Reaction. *J. Am. Chem. Soc.* **2019**, *141*, 16255–16259. (b) Hensel, T.; Andersen, N. N.; Plesner, M.; Pittelkow, M. Synthesis of Heterocyclic [8]Circulenes and Related Structures. *Synlett* **2016**, *27*, 498–525. (c) Kawahara, K. P.; Matsuoka, W.; Ito, H.; Itami, K. Synthesis of Nitrogen-Containing Polyaromatics by Aza-Annulative π -Extension of Unfunctionalized Aromatics. *Angew. Chem., Int. Ed.* **2020**, *59*, 6383–6388. (d) Stepek, I. A.; Itami, K. Recent Advances in C-H Activation for the Synthesis of π -Extended Materials. *ACS Mater. Lett.* **2020**, *2*, 951–974. (e) Martin, M. M.; Lungerich, D.; Haines, P.; Hampel, F.; Jux, N. Electronic Communication across Porphyrin Hexabenzocoronene Isomers. *Angew. Chem., Int. Ed.* **2019**, *58*, 8932–8937.
- (3) Mitsudo, K.; Matsuo, R.; Yonezawa, T.; Inoue, H.; Mandai, H.; Suga, S. Electrochemical Synthesis of Thienoacene derivatives: Transition-Metal-Free Dehydrogenative C-S Coupling Promoted by a Halogen Mediator. *Angew. Chem., Int. Ed.* **2020**, *59*, 7803–7807.
- (4) Wetzel, Ch.; Brier, E.; Vogt, A.; Mishra, A.; Mena-Osteritz, E.; Bäuerle, P. Fused Thiophene-Pyrrole-Containing Ring Systems up to a Heterodecacene. *Angew. Chem., Int. Ed.* **2015**, *54*, 12334–12338.
- (5) Zhao, M.; Zhang, B.; Miao, Q. Revisiting Indolo[3,2-b]carbazole: Synthesis, Structures, Properties and Applications. *Angew. Chem., Int. Ed.* **2020**, *59*, 9678–9683.
- (6) Zheng, T.; Cai, Z.; Ho-Wu, R.; Yau, S. H.; Shaparov, V.; Goodson, T.; Yu, L. Synthesis of Ladder-Type Thienoacenes and Their Electronic and Optical Properties. *J. Am. Chem. Soc.* **2016**, *138*, 868–875.
- (7) Tsutsui, Y.; Schweicher, G.; Chattopadhyay, B.; Sakurai, T.; Arlin, J.-B.; Ruzié, C.; Aliev, A.; Ciesielski, A.; Colella, S.; Kennedy, A. R.; Lemaire, V.; Olivier, Y.; Hadji, R.; Sanguinet, L.; Castet, F.; Osella, S.; Dudenko, D.; Beljonne, D.; Cornil, J.; Samori, P.; Seki, S.; Geerts, Y. H. Unraveling Unprecedented Charge Carrier Mobility through Structure

Property Relationship of Four Isomers of Didodecyl[1]benzothieno[3,2-b][1]benzothiophene. *Adv. Mater.* **2016**, *28*, 7106–7114.

(8) Schweicher, G.; Lemaury, V.; Niebel, C.; Ruzié, C.; Diao, Y.; Goto, O.; Lee, W.-Y.; Kim, Y.; Arlin, J.-B.; Karpinska, J.; Kennedy, A. R.; Parkin, S. R.; Olivier, Y.; Mannsfeld, S. C. B.; Cornil, J.; Geerts, Y. H.; Bao, Z. Bulky End-Capped [1]benzothieno[3,2-b]benzothiophenes: Reaching High-Mobility Organic Semiconductors by Fine Tuning of the Crystalline Solid-State Order. *Adv. Mater.* **2015**, *27*, 3066–3072.

(9) Abe, M.; Mori, T.; Osaka, I.; Sugimoto, K.; Takimiya, K. Thermally, Operationally, and Environmentally Stable Organic Thin-Film Transistors Based on Bis[1]benzothieno[2,3-d:2',3'-d']naphtho[2,3-b:6,7-b']dithiophene Derivatives: Effective Synthesis, Electronic Structures, and Structure–Property Relationship. *Chem. Mater.* **2015**, *27*, 5049–5057.

(10) Wang, W.; Lu, H.; Chen, Z.; Jia, B.; Li, K.; Ma, W.; Zhan, X. High-Performance NIR-Sensitive Fused Tetrathienoacene Electron Acceptors. *J. Mater. Chem. A* **2020**, *8*, 3011–3017.

(11) Qin, R.; Wang, D.; Zhou, G.; Yu, Z.-P.; Li, S.; Li, Y.; Liu, Z.-X.; Zhu, H.; Shi, M.; Lu, X.; Li, Ch.-Z.; Chen, H. Tuning Terminal Aromatics of Electron Acceptors to Achieve High-Efficiency Organic Solar Cells. *J. Mater. Chem. A* **2019**, *7*, 27632–27639.

(12) Goujon, A.; Colom, A.; Straková; Karolina Mercier, V.; Mahecic, D.; Manley, S.; Sakai, N.; Roux, A.; Matile, S. Mechanosensitive Fluorescent Probest o Image Membrane Tension in Mitochondria, Endoplasmic Reticulum, and Lysosomes. *J. Am. Chem. Soc.* **2019**, *141*, 3380–3384.

(13) (a) Poronik, Y. M.; Mazur, L. M.; Samoć, M.; Jacquemin, D.; Gryko, D. T. 2,5-Bis(azulenyl)pyrrolo[3,2-b]pyrroles – the key influence of the linkage position on the linear and non-linear optical properties. *J. Mater. Chem. C* **2017**, *5*, 2620–2628. (b) Banasiewicz, M.; Stężycki, R.; Kumar, D. G.; Krzeszewski, M.; Tasiór, M.; Koszarna, B.; Janiga, A.; Vakuliuk, O.; Sadowski, B.; Gryko, D. T.; Jacquemin, D. Electronic Communication in Pyrrolo[3,2-b]pyrroles Possessing Sterically Hindered Aromatic Substituents. *Eur. J. Org. Chem.* **2019**, *2019*, 5247–5253. (c) Friese, D. H.; Mikhaylov, A.; Krzeszewski, M.; Poronik, Y. M.; Rebane, A.; Ruud, K.; Gryko, D. T. Pyrrolo[3,2-b]pyrroles—From Unprecedented Solvatochromism to Two-Photon Absorption. *Chem. – Eur. J.* **2015**, *21*, 18364–18374. (d) Krzeszewski, M.; Kodama, T.; Espinoza, E. M.; Vullev, V. I.; Kubo, T.; Gryko, D. T. Nonplanar Butterfly-Shaped π -Expanded Pyrrolopyrroles. *Chem. – Eur. J.* **2016**, *22*, 16478–16488. (e) Krzeszewski, M. K.; Gryko, D.; Gryko, D. T. The Tetraarylpyrrolo[3,2-b]pyrroles-From Serendipitous Discovery to Promising Heterocyclic Optoelectronic Materials. *Acc. Chem. Res.* **2017**, *50*, 2334–2345. and references cited therein.

(14) (a) Janiga, A.; Glodkowska-Mrowka, E.; Stoklosa, T.; Gryko, D. T. Synthesis and Optical Properties of Tetraaryl-1,4-Dihydropyrrolo[3,2-b]pyrroles. *Asian J. Org. Chem.* **2013**, *2*, 411–415. (b) Krzeszewski, M.; Thorsted, B.; Brewer, J.; Gryko, D. T. Tetraaryl-, Pentaaryl-, and Hexaaryl-1,4-Dihydropyrrolo[3,2-b]pyrroles: Synthesis and Optical Properties. *J. Org. Chem.* **2014**, *79*, 3119–3128.

(15) Ivanov, A. I.; Dereka, B.; Vauthey, E. A Simple Model of Solvent-Induced Symmetry-Breaking Charge Transfer in Excited Quadrupolar Molecules. *J. Chem. Phys.* **2017**, *146*, No. 164306.

(16) Liu, H.; Ye, J.; Zhou, Yu.; Fu, L.; Lu, Q.; Zhang, C. New Pyrrolo[3,2-b]pyrrole Derivatives with Multiple-Acceptor Substitution: Efficient Fluorescent Emission and Near-Infrared Two-Photon Absorption. *Tetrahedron Lett.* **2017**, *58*, 4841–4844.

(17) Dereka, B.; Vauthey, E. Direct Local Solvent Probing by Transient Infrared Spectroscopy Reveals the Mechanism of Hydrogen-Bond Induced Nonradiative Deactivation. *Chem. Sci.* **2017**, *8*, 5057–5066.

(18) Wu, J.-Y.; Yu, C.-H.; Wen, J.-J.; Chang, C.-L.; Leung, M. Pyrrolo[3,2-b]pyrroles for Photochromic Analysis of Halocarbons. *Anal. Chem.* **2016**, *88*, 1195–1201.

(19) Zhao, B.; Xu, Y.; Liu, S.; Li, C.; Fu, N.; Wang, L. Non-Fullerene Receptor Material Based on Tetraarylpyrrole Nuclear and Its Application in Organic Solar Cell Device. CN108912125A, 2018.

(20) Wang, J.; Chai, Z.; Liu, S.; Fang, M.; Chang, K.; Han, M.; Hong, L.; Han, H.; Li, Q.; Li, Z. Organic Dyes Based on Tetraaryl-1,4-dihydropyrrolo[3,2-b]pyrroles for Photovoltaic and Photocatalysis Applications with the Suppressed Electron Recombination. *Chem. – Eur. J.* **2018**, *24*, 18032–18042.

(21) Domínguez, R.; Montcada, N. F.; de la Cruz, P.; Palomares, E.; Langa, F. Pyrrolo[3,2-b]pyrrole as the Central Core of the Electron Donor for Solution-Processed Organic Solar Cells. *ChemPlusChem* **2017**, *82*, 1096–1104.

(22) Zhou, Y.; Zhang, M.; Ye, J.; Liu, H.; Wang, K.; Yuan, Y.; Du, Y.-Q.; Zhang, C.; Zheng, C.-J.; Zhang, X.-H. Efficient Solution-Processed Red Organic Light-Emitting Diode Based on an Electron-Donating Building Block of Pyrrolo[3,2-b]pyrrole. *Org. Electron.* **2019**, *65*, 110–115.

(23) Canjeevaram Balasubramanyam, R. K.; Kumar, R.; Ippolito, S. J.; Bhargava, S. K.; Periasamy, S. R.; Narayan, R.; Basak, P. Quadrupolar (A- π -D- π -A) Tetra-Aryl 1,4-Dihydropyrrolo[3,2-b]Pyrroles as Single Molecular Resistive Memory Devices: Substituent Triggered Amphoteric Redox Performance and Electrical Bistability. *J. Phys. Chem. C* **2016**, *120*, 11313–11323.

(24) (a) Ji, Y.; Peng, Z.; Tong, B.; Shi, J.; Zhi, J.; Dong, Y. Polymorphism-Dependent Aggregation-Induced Emission of Pyrrolopyrrole-Based Derivative and Its Multi-Stimuli Response Behaviors. *Dyes Pigm.* **2017**, *139*, 664–671. (b) Li, K.; Liu, Y.; Li, Y.; Feng, Q.; Hou, H.; Tang, B. Z. 2,5-Bis(4-alkoxycarbonylphenyl)-1,4-diaryl-1,4-dihydropyrrolo[3,2-b]pyrrole (AAPP) AIEgens: Tunable RIR and TICT Characteristics and Their Multifunctional Applications. *Chem. Sci.* **2017**, *8*, 7258–7267. (c) Ma, Y.; Zhang, Y.; Kong, L.; Yang, J. Mechanoresponsive Material of AIE-Active 1,4-Dihydropyrrolo[3,2-b]pyrrole Luminophores Bearing Tetraphenylethylene Group with Rewritable Data Storage. *Molecules* **2018**, *23*, 3255.

(25) Hawes, C. S.; O Máille, G. M.; Byrne, K.; Schmitt, W.; Gunnlaugsson, T. Tetraarylpyrrolo[3,2-b]pyrroles as Versatile and Responsive Fluorescent Linkers in Metal–Organic Frameworks. *Dalton Trans.* **2018**, *47*, 10080–10092.

(26) Wu, D.; Zheng, J.; Xu, C.; Kang, D.; Hong, W.; Duan, Z.; Mathey, F. Phosphindole Fused Pyrrolo[3,2-b]pyrroles: A New Single-Molecule Junction for Charge Transport. *Dalton Trans.* **2019**, *48*, 6347–6352.

(27) Tasiór, M.; Koszarna, B.; Young, D. C.; Bernard, B.; Jacquemin, D.; Gryko, D.; Gryko, D. T. Fe(III)-Catalyzed Synthesis of Pyrrolo[3,2-b]pyrroles: Formation of New Dyes and Photophysical Studies. *Org. Chem. Front.* **2019**, *6*, 2939–2948.

(28) Martins, L. M.; de Faria Vieira, S.; Baldacim, G. B.; Bregadiolli, B. A.; Caraschi, J. C.; Batagin-Neto, A.; Silva-Filho, L. C. Improved synthesis of tetraaryl-1,4-dihydropyrrolo[3,2-b]pyrroles a promising dye for organic electronic devices: An experimental and theoretical approach. *Dyes Pigm.* **2018**, *148*, 81.

(29) Krzeszewski, M.; Sahara, K.; Poronik, Y. M.; Kubo, T.; Gryko, D. T. Unforeseen 1,2-Aryl Shift in Tetraarylpyrrolo[3,2-b]pyrroles Triggered by Oxidative Aromatic Coupling. *Org. Lett.* **2018**, *20*, 1517–1520.

(30) (a) Yang, W.; Monteiro, J. H. S. K.; de Bettencourt-Dias, A.; Catalano, V. J.; Chalifoux, W. A. Pyrenes, Peropyrenes, and Teropyrenes: Synthesis, Structures, and Photophysical Properties. *Angew. Chem. Int. Ed.* **2016**, *55*, 10427–10430. (b) Yang, W.; Kazemi, R. R.; Karunathilake, N.; Catalano, V. J.; Alpuche-Aviles, M. A.; Chalifoux, W. A. Expanding the scope of peropyrenes and teropyrenes through a facile InCl₃-catalyzed multifold alkyne benzannulation. *Org. Chem. Front.* **2018**, *5*, 2288–2295.

(31) Krzeszewski, M.; Świder, P.; Dobrzycki, Ł.; Cyrański, M.; Danikiewicz, W.; Gryko, D. T. The role of steric hindrance in intramolecular oxidative aromatic coupling of pyrrolo[3,2-b]pyrroles. *Chem. Commun.* **2016**, *52*, 11539–11542.

(32) (a) Noland, W. E.; Kuryla, W. C.; Lange, R. F. The Synthesis of Carbazoles from 3-Vinylindoles with Tetracyanoethylene and Dimethyl Acetylenedicarboxylate. *J. Am. Chem. Soc.* **1959**, *81*, 6010–6017. (b) Michinobu, T.; Diederich, F. The [2+2] Cycloaddition-Retroelectrocyclization (CA-RE) Click Reaction: Facile Access to Molecular and Polymeric Push-Pull Chromophores. *Angew. Chem., Int.*

Ed. **2018**, *57*, 3552–3577. (c) Fatiadi, A. J. New applications of tetracyanoethylene in organic chemistry. *Synthesis* **1986**, *1986*, 249–284.

(33) Radtke, J.; Møllerup, S. M.; Bolte, M.; Lerner, H.-W.; Wang, S.; Wagner, M. Aryl Insertion vs Aryl–Aryl Coupling in C,C-Chelated Organoborates: The “Missing Link” of Tetraarylborate Photochemistry. *Org. Lett.* **2018**, *20*, 3966–3970.

(34) Domínguez, Z.; Pais, V. F.; Collado, D.; Vázquez-Domínguez, P.; Albendín, F. N.; Pérez-Inestrosa, E.; Ros, A.; Pischel, U. π -Extended Four-Coordinate Organoboron N,C-Chelates as Two-Photon Absorbing Chromophores. *J. Org. Chem.* **2019**, *84*, 13384–13393.

(35) Pais, V. F.; Alcaide, M. M.; Lúpez-Rodríguez, R.; Collado, D.; Nájera, F.; Pérez-Inestrosa, E.; Álvarez, E.; Lassaletta, J. M.; Fernández, R.; Ros, A.; Pischel, U. Strongly Emissive and Photostable Four-Coordinate Organoboron N,C Chelates and Their Use in Fluorescence Microscopy. *Chem. – Eur. J.* **2015**, *21*, 15369–15376.

(36) Górski, K.; Mech-Piskorz, J.; Noworyta, K.; Leśniewska, B.; Pietraszkiewicz, M. Efficient Synthesis of 5-Oxatruene and the Unusual Influence of Oxygen Heteroatom on Its Physico-Chemical Properties. *New J. Chem.* **2018**, *42*, 5844–5852.

(37) Krystkowiak, E.; Dobek, K.; Maciejewski, A. An intermolecular hydrogen-bonding effect on spectra and photophysical properties of 6-aminocoumarin in protic solvents. *Photochem. Photobiol. Sci.* **2013**, *12*, 446–455.